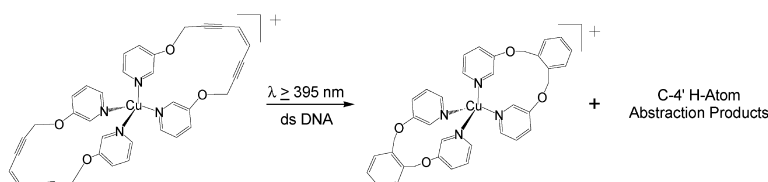Article

Metal–Ligand Charge-Transfer-Promoted Photoelectronic Bergman Cyclization of Copper Metalloenediynes: Photochemical DNA Cleavage via C-4' H-Atom Abstraction

Pedro J. Benites, Rebecca C. Holmberg, Diwan S. Rawat, Brian J. Kraft,
Lee J. Klein, Dennis G. Peters, H. Holden Thorp, and Jeffrey M. Zaleski

More About This Article

Additional resources and features associated with this article are available within the HTML version:

- Supporting Information
- Links to the 10 articles that cite this article, as of the time of this article download
- Access to high resolution figures
- Links to articles and content related to this article
- Copyright permission to reproduce figures and/or text from this article

View the Full Text HTML

Metal−Ligand Charge-Transfer-Promoted Photoelectronic Bergman Cyclization of Copper Metalloenediynes: Photochemical DNA Cleavage via C-4′ H-Atom Abstraction

Pedro J. Benites,[†] Rebecca C. Holmberg,[‡] Diwan S. Rawat,[†] Brian J. Kraft,[†]
Lee J. Klein,[†] Dennis G. Peters,[†] H. Holden Thorp,*,[‡] and Jeffrey M. Zaleski*,[†]

*Contribution from the Department of Chemistry, Indiana University,
Bloomington, Indiana 47405, and Department of Chemistry, Venable Hall,
University of North Carolina, Chapel Hill, North Carolina 27599-3290*

Received July 9, 2002; E-mail: zaleski@indiana.edu

Abstract: Metal-to-ligand charge-transfer (MLCT) photolyses ($\lambda \geq 395$ nm) of copper complexes of *cis*-1,8-bis(pyridin-3-oxy)oct-4-ene-2,6-diyne (bpod, **1**), [Cu(bpod)$_2$]PF$_6$ (**2**), and [Cu(bpod)$_2$](NO$_3$)$_2$ (**3**) yield Bergman cyclization of the bound ligands. In contrast, the uncomplexed ligand **1** and Zn(bpod)$_2$(CH$_3$COO)$_2$ compound (**4**) are photochemically inert under the same conditions. In the case of **4**, sensitized photochemical generation of the lowest energy $^3\pi-\pi^*$ state, which is localized on the enediyne unit, leads to production of the *trans*-bpod ligand bound to the Zn(II) cation by photoisomerization. Electrochemical studies show that **1**, both the uncomplexed and complexed, exhibits two irreversible waves between E_p values of -1.75 and -1.93 V (vs SCE), corresponding to reductions of the alkyne units. Irreversible, ligand-based one-electron oxidation waves are also observed at $+1.94$ and $+2.15$ V (vs SCE) for **1** and **3**. Copper-centered oxidation of **2** and reduction of **3** occur at $E_{1/2} = +0.15$ and $+0.38$ V, respectively. Combined with the observed Cu(I)-to-pyridine(π^*) MLCT and pyridine(π^*)-to-Cu(II) ligand-to-metal charge transfer (LMCT) absorption centered near $\sim$315 nm, the results suggest a mechanism for photo-Bergman cyclization that is derived from energy transfer to the enediyne unit upon charge-transfer excitation. The intermediates produced upon photolysis degrade both pUC19 bacterial plasmid DNA, as well as a 25-base-pair, double-stranded oligonucleotide. Detailed analyses of the cleavage reactions reveal 5′-phosphate and 3′-phosphoglycolate termini that are derived from H-atom abstraction from the 4′-position of the deoxyribose ring rather than redox-induced base oxidation.

1. Introduction

The ability to control Bergman cyclization of enediyne compounds photochemically with variable-wavelength electronic excitation leads to potential applications of these unique molecules in photodynamic therapy[1−4] and biomedicine[5−9] or as diagnostic tools for molecular biology.[10] The chemical feature that distinguishes these molecules from their biologically active counterparts is their unique 1,5-diyn-3-ene unit,[11−16] which rearranges to form a potent 1,4-phenyl diradical intermediate without the need for external cofactors or reagents. The unusual capability of these molecular structures to generate a toxic diradical intermediate unimolecularly warrants their continued examination in an effort to develop well-controlled initiation of Bergman cyclization reactivity.

The use of electronic excitation to activate thermally stable enediyne structures photochemically is a direct response to the problem of controlled initiation. Indeed, it has been known for some time that both enediyne natural products[17,18] and synthetic

† Indiana University.
‡ University of North Carolina.

(1) Boyle, R. W.; Dolphin, D. *Photochem. Photobiol.* **1996**, *64*, 469−485.
(2) Mody, T. M.; Sessler, J. L., Eds. *Supramolecular Materials and Technologies*; Wiley: Chichester, U.K., 1999; Vol. 4.
(3) Ali, H.; van Lier, J. E. *Chem. Rev.* **1999**, *99*, 2379−2450.
(4) Bonnett, R.; Martinez, G. *Tetrahedron* **2001**, *57*, 9513−9547.
(5) Abramson, A. L.; Shikowitz, M. J.; Mullooly, V. M.; Steinberg, B. M.; Amella, C. A.; Rothstein, H. R. *Arch. Otolaryngol., Head Neck Surg.* **1992**, *118*, 25−29.
(6) Sieber, F.; O'Brien, J. M.; Gaffney, D. K. *Blood Cells* **1992**, *18*, 117−128.
(7) Sieber, F.; O'Brien, J. M.; Gaffney, D. K. *Semin. Hematol.* **1992**, *29*, 79−87.
(8) Matthews, J. L.; Sogandares-Bernal, F.; Judy, M.; Gulliya, K.; Newman, J.; Chanh, T.; Marengo-Rowe, A. *Blood Cells* **1992**, *18*, 75−89.
(9) North, J.; Neyndorff, H.; Lewis, J. G. *J. Photochem. Photobiol. B* **1993**, *17*, 99−108.
(10) Tullius, T. D. In *Metal−DNA Chemistry*; Tullius, T. D., Ed.; American Chemical Society: Washington, DC, 1989; Vol. 402, pp 1−23.

(11) Lee, M. D.; Dunne, T. S.; Siegal, M. M.; Chang, C. C.; Morton, G. O.; Borders, D. B. *J. Am. Chem. Soc.* **1987**, *109*, 3464−3466.
(12) Lee, M. D.; Dunne, T. S.; Chang, C. C.; Ellestad, G. A.; Siegal, M. M.; Morton, G. O.; McGahren, W. J.; Borders, D. B. *J. Am. Chem. Soc.* **1987**, *109*, 3466−3468.
(13) Lee, M. D.; Dunne, T. S.; Chang, C. C.; Siegal, M. M.; Morton, G. O.; Ellestad, G. A.; McGahren, W. J.; Borders, D. B. *J. Am. Chem. Soc.* **1992**, *114*, 985−997.
(14) Konishi, M.; Ohkuma, H.; Tsuno, T.; Oki, T.; VanDuyne, G. D.; Clardy, J. *J. Am. Chem. Soc.* **1989**, *112*, 3715−3716.
(15) Golik, J.; Clardy, J.; Dubay, G.; Groenewold, G.; Kawaguchi, H.; Konishi, M.; Krishnan, B.; Ohkuma, H.; Saitoh, K.; Doyle, T. W. *J. Am. Chem. Soc.* **1987**, *109*, 3461−3462.
(16) Golik, J.; Clardy, J.; Dubay, G.; Groenewold, G.; Kawaguchi, H.; Konishi, M.; Krishnan, B.; Ohkuma, H.; Saitoh, K.; Doyle, T. W. *J. Am. Chem. Soc.* **1987**, *109*, 3462−3464.
(17) Uesawa, Y.; Kuwahara, J.; Sugiura, Y. *Biochem. Biophys. Res. Commun.* **1989**, *164*, 903−911.
(18) Sugiura, Y.; Shiraki, T.; Konishi, M.; Oki, T. *Proc. Natl. Acad. Sci. U.S.A.* **1990**, *87*, 3831−3835.

analogues[19−26] can be photochemically activated to generate fully cyclized Bergman products upon UV excitation. Recently, the kinetics[22] and electronic structures of enediyne excited states[27] giving rise to the observed product distributions, have been more clearly elucidated. The emerging theme for photo-Bergman cyclization of simple organic enediyne ligands is that photoexcitation leads to an alkyne-localized excited $^1\pi-\pi^*$ state that promotes an in-plane geometric distortion, leading to the Bergman-cyclized 1,4-phenyl diradical intermediate.[27] In contrast, population of the lowest-energy $^3\pi-\pi^*$ state, which is localized on the ene functionality, leads to the potential for an out-of-plane geometric distortion via rotation about the double bond and localization of unpaired electron density at the alkyne termini. This leads to sites for H-atom abstraction and the subsequent formation of dien-yne photoproducts.

Binding of transition-metal ions to simple enediyne ligands influences thermal Bergman cyclization temperatures by inducing a geometry that approaches the transition-state structure, thereby lowering the activation barrier to cycloaromatization.[28−41] However, the potential role of metal ions in photo-Bergman cyclization reactivity has not been examined. It is well established that photochemical activation of both σ- and π-bound metal complexes can lead to ligand dissociation and/or photoreduction reactions.[42] In the case of simple organic enediynes, ligand-centered redox chemistry does not lead to 1,6-Bergman cyclization. Rather, 1,5-cyclization and subsequent ion-radical reactions are observed.[43] Thus, it is unclear at first glance how transition metals, especially those that are redox active, may participate in driving photoinduced Bergman cyclization.

One electronic property that redox-active transition-metal complexes exhibit is the presence of metal-to-ligand charge-transfer (MLCT) absorption bands in the optical spectrum. These transitions are derived from significant spatial overlap between the metal dσ or dπ molecular orbitals and bound ligand σ or π molecular orbitals. The presence of such absorption features, however, does not mandate that the participating metal- or ligand-centered orbitals be the highest occupied molecular orbital (HOMO) or the lowest unoccupied molecular orbital (LUMO) of the complex. These localized states can therefore serve as pathways to reactive electronic configurations that do not absorb photons in the ground state (e.g., long-range charge-separated states) and, therefore, are not populated directly by optical excitation.[44−46] Conceptually, this could lead to new design strategies that utilize MLCT absorption to initiate Bergman cyclization with visible-region photons photochemically, which would relax the requirement for high-energy, alkyne-localized electronic excitation to drive such reactions.

Beyond the excited-state mechanistic details of photoinitiated Bergman cyclization, the ability of the potent 1,4-phenyl diradical intermediate to perform DNA degradation via H-atom abstraction rather than redox reactions gives these metalloenediynes potential advantages over other metal-activated thermal or photochemical agents. Thermal and photochemical DNA cleavage[47,48] by transition-metal complexes frequently occurs by one of three general mechanisms: (i) one-electron guanine oxidation (e.g., Ni(II) peptide[49,50] and macrocycle[50−54] complex reactions with $KHSO_5$, $Cr_2O_7^{2-}/H_2O_2$,[55] $CuCl_2/H_2O_2$,[56−58] $ReO_2(4\text{-OMepy})_4^+$,[59] $Ru(bpy)_3^{3+}$,[60,61] and $[Co(NH_3)_6]^{3+}$ via $^1O_2$[62]), (ii) oxygen-atom transfer oxidation (e.g., $[Ru(IV)(tpy)(bpy)O]^{2+}$,[63] $[Ru(III)(tpy)(bpy)OH]^{2+}$,[64]) and sugar degradation by H-atom abstraction (e.g., Fe(II)-bleomycin,[65] Rh-phi complexes,[66] and $[Cu(phen)_2]^+$ complexes[67]). The most common of these is nucleobase oxidation at G-sites that is due to the relatively low redox potential for guanine oxidation, as well as

(19) von Nicolaou, K. C.; Dai, W.-M.; Wendeborn, S. V.; Smith, A. L.; Torisawa, Y.; Maligres, P.; Hwang, C.-K. *Angew. Chem., Int. Ed. Engl.* **1991**, *30*, 1032−1036.
(20) Wender, P. A.; Zercher, C. K.; Beckham, S.; Haubold, E.-M. *J. Org. Chem.* **1993**, *58*, 5867−5869.
(21) Funk, R. L.; Young, E. R. R.; Williams, R. M.; Flanagan, M. F.; Cecil, T. L. *J. Am. Chem. Soc.* **1996**, *118*, 3291−3292.
(22) Evenzahav, A.; Turro, N. J. *J. Am. Chem. Soc.* **1998**, *120*, 1835−1841.
(23) Kaneko, T.; Takahashi, M.; Hirama, M. *Angew. Chem., Int. Ed.* **1999**, *38*, 1267−1268.
(24) Choy, N.; Blanco, B.; Wen, J.; Krishan, A.; Russell, K. C. *Org. Lett.* **2000**, *2*, 3761−3764.
(25) Jones, G. B.; Wright, J. M.; Plourde, G., II.; Purohit, A. D.; Wyatt, J. K.; Hynd, G.; Fouad, F. *J. Am. Chem. Soc.* **2000**, *122*, 9872−9873.
(26) Purohit, A.; Wyatt, J.; Hynd, G.; Wright, J.; El-Shafey, A.; Swamy, N.; Ray, R.; Jones, G. B. *Tetrahedron Lett.* **2001**, *42*, 8579−8582.
(27) Clark, A. L.; Davidson, E. R.; Zaleski, J. M. *J. Am. Chem. Soc.* **2001**, *123*, 2650−2657.
(28) Warner, B. P.; Millar, S. P.; Broene, R. D.; Buchwald, S. L. *Science* **1995**, *269*, 814−816.
(29) Konig, B.; Pitsch, W.; Thondorf, I. *J. Org. Chem.* **1996**, *61*, 4258−4261.
(30) Basak, A.; Shain, J. C. *Tetrahedron Lett.* **1998**, *39*, 3029−3030.
(31) Basak, A.; Shain, J. C.; Khamari, U. K.; Rudra, K. R.; Basak, A. *J. Chem. Soc., Perkin Trans. 1* **2000**, 1955−1964.
(32) Basak, A.; Rudra, K. R. *Tetrahedron Lett.* **2000**, *41*, 7231−7234.
(33) Basak, A.; Bdour, H. M.; Shain, J. C.; Mandal, S.; Rudra, K. R.; Nag, S. *Bioorg. Med. Chem. Lett.* **2000**, *10*, 1321−1325.
(34) Coalter, N.; Concolino, T. E.; Streib, W. E.; Hughes, C. G.; Rheingold, A. L.; Zaleski, J. M. *J. Am. Chem. Soc.* **2000**, *122*, 3112−3117.
(35) Benites, P. J.; Rawat, D. S.; Zaleski, J. M. *J. Am. Chem. Soc.* **2000**, *122*, 7208−7217.
(36) Konig, B. *Eur. J. Org. Chem.* **2000**, 381−385.
(37) O'Connor, J. M.; Lee, L. I.; Gantzel, P.; Rheingold, A. L.; Lam, K.-C. *J. Am. Chem. Soc.* **2000**, *122*, 12057−12058.
(38) Rawat, D. S.; Benites, P. J.; Incarvito, C. D.; Rheingold, A. L.; Zaleski, J. M. *Inorg. Chem.* **2001**, *40*, 1846−1857.
(39) Schmitt, E. S.; Huffman, J. C.; Zaleski, J. M. *Chem. Commun.* **2001**, 167−168.
(40) O'Connor, J. M.; Friese, S. J.; Tichenor, M. *J. Am. Chem. Soc.* **2002**, *124*, 3506−3507.
(41) Rawat, D. S.; Zaleski, J. M. *Synth. Commun.* **2002**, *32*, 1489−1494.
(42) Horvath, O.; Stevenson, K. L. *Charge-Transfer Photochemistry of Coordination Compounds*; VCH: New York, 1993; p 380.
(43) Ramkumar, D.; Kalpana, M.; Varghese, B.; Sankararaman, S.; Jagadeesh, M. N.; Chandrasekhar, J. *J. Org. Chem.* **1996**, *61*, 2247−2250.
(44) Balzani, V.; Scandola, F. *Supramolecular Photochemistry*; Ellis Horwood: New York, 1991.
(45) Vlcek, A. *Coord. Chem. Rev.* **1998**, *177*, 219−256.
(46) Ramamurthy, V., Schanze, K. S., Eds. *Organic and Inorganic Photochemistry*; Marcel Dekker: New York, 1998; Vol. 2.
(47) Burrows, C. J.; Muller, J. G. *Chem. Rev.* **1998**, *98*, 1109−1152.
(48) Armitage, B. *Chem. Rev.* **1998**, *98*, 1171−1200.
(49) Liang, Q.; Ananias, D. C.; Long, E. C. *J. Am. Chem. Soc.* **1998**, *120*, 248−257.
(50) Muller, J. G.; Hickerson, R. P.; Perez, R. J.; Burrows, C. J. *J. Am. Chem. Soc.* **1997**, *119*, 1501−1506.
(51) Muller, J. G.; Zheng, P.; Rokita, S. E.; Burrows, C. J. *J. Am. Chem. Soc.* **1996**, *118*, 2320−2325.
(52) Chen, X.; Burrows, C. J.; Rokita, S. E. *J. Am. Chem. Soc.* **1992**, *114*, 322−325.
(53) Muller, J. G.; Chen, X.; Dadiz, A. C.; Rokita, S. E.; Burrows, C. J. *J. Am. Chem. Soc.* **1992**, *114*, 6407−6411.
(54) Burrows, C. J.; Rokita, S. E. *Acc. Chem. Res.* **1994**, *27*, 295−301.
(55) Misra, M.; Alcedo, K. J. A.; Wetterhahn, K. E. *Carcinogenesis* **1994**, *15*, 2911−2917.
(56) Yamamoto, K.; Kawanishi, S. *J. Biol. Chem.* **1989**, *264*, 15435−15440.
(57) Yamamoto, K.; Kawanishi, S. *J. Biol. Chem.* **1991**, *266*, 1509−1515.
(58) Oikawa, S.; Kawanishi, S. *Biochemistry* **1996**, *35*, 4584−4590.
(59) Johnston, D. H.; Cheng, C.-C.; Campbell, K. J.; Thorp, H. H. *Inorg. Chem.* **1994**, *33*, 6388−6390.
(60) Fedorova, O. S.; Podust, L. M. *J. Inorg. Biochem.* **1988**, *34*, 149−155.
(61) Gorner, H.; Stradowski, C.; Schulte-Frolinde, D. *Photochem. Photobiol.* **1988**, *47*, 15−29.
(62) Yamamoto, K.; Inoue, S.; Yamazaki, A.; Yoshinaga, T.; Kawanishi, S. *Chem. Res. Toxicol.* **1989**, *2*, 234−239.
(63) Carter, P. J.; Cheng, C.-C.; Thorp, H. H. *Inorg. Chem.* **1996**, *35*, 3348−3354.
(64) Cheng, C. C.; Goll, J. G.; Neyhart, G. A.; Welch, T. W.; Singh, P.; Thorp, H. H. *J. Am. Chem. Soc.* **1995**, *117*, 2970−2980.
(65) Stubbe, J.; Kozarich, J. W. *Chem. Rev.* **1987**, *87*, 1107−1136.
(66) Pyle, A. M.; Long, E. C.; Barton, J. K. *J. Am. Chem. Soc.* **1989**, *111*, 4520−4522.
(67) Sigman, D. S.; Bruice, T. W.; Mazumder, A.; Sutton, C. L. *Acc. Chem. Res.* **1993**, *26*, 98−104.

the ability of transition metals to bind to N7. Reactions such as FeEDTA/H_2O_2[68] or $CuCl_2^{2+}$/H_2O_2[69] that generate •OH or Mn(V)-oxo intermediates[70,71] formed by two-electron oxidation can perform both ribose and nucleobase oxidation. However, the potential to generate freely diffusing •OH with such reagents can lead to reduced specificity. Thus, it would be potentially beneficial to have molecules that can be activated with visible excitation to produce localized radicals that could perform site-directed H-atom abstraction rather than thermodynamically determined base oxidation. Overall, such approaches may lead to reagents with improved specificity, where recognition is determined solely by the targeting element.

Within this theme, we report the photoelectronic Bergman cyclization of copper metalloenediynes via MLCT excitation. The photochemical products from these reactions show good yields of the cycloaromatized ligand, indicating that the reaction is not a consequence of irreversible redox chemistry. These reactivities are in contrast to those observed upon photolysis of the free ligand or the Zn^{2+} analogue, suggesting that MLCT excitation plays an important role in these photoreactions. Moreover, we show that the intermediates produced upon photolysis are potent to degrade both bacterial plasmid DNA and a 25-base-pair (25-bp), double-stranded oligonucleotide. The cleavage products derived from the oligonucleotide are indicative of H-atom abstraction from the deoxyribose ring and not base oxidation.

2. Experimental Section

2.1. Syntheses and Photochemistry. 2.1.1. Materials. All preparations were performed under a nitrogen atmosphere, using standard Schlenk and drybox techniques. Acetonitrile and dichloromethane were dried and distilled from calcium hydride. Dichloromethane and dimethylformamide (DMF) were stored over 4 Å molecular sieves. The acetonitrile used was HPLC grade, whereas the methanol, ether, and isopropyl alcohol used were spectroscopic grade. NMR solvents (acetonitrile-d_3, dimethylsulfoxide-d_6 (DMSO-d_6), and chloroform-d_3) were dried over activated 3 Å and 4 Å molecular sieves and degassed by bubbling with nitrogen for 30 min. Degassed spectroscopic-grade solvents were used for all UV−Vis measurements. All chemicals used in the syntheses of all metalloenediynes were of the highest purity available and were obtained from Aldrich and Fluka and used as received. The organic enediyne compounds and photoproducts were purified by flash chromatography with 60 Å silica gel (430−230 μm) using HPLC-grade hexanes, ethyl acetate, dichloromethane, and methanol.

2.1.2. Physical Measurements. ^{1}H and ^{13}C NMR were recorded on a Varian model VXR400 NMR spectrometer. The multiplicity of the ^{13}C signals was determined by the DEPT technique. High-resolution electron ionization (EI) and fast ion bombardment (FAB) mass spectroscopy (MS) spectra were acquired on a Kratos model MS-80 mass spectrometer that was interfaced with a Kratos model DS90 data system. ESI-MS data were obtained at the University of Illinois with a Micromass Quattro I mass spectrometer, and elemental analyses on the samples were obtained from Atlantic Microlab, Inc. Photolyses were performed using a 1000-W XeHg lamp (Oriel model 66021) at λ ≥ 320, 345, or 395 nm, where the cutoff wavelengths were selected using a series of long-wavelength-pass Schott filters (Oriel 51872). Samples

were contained in either anaerobic (Kontes) quartz tubes or Pyrex J-Young NMR tubes (the outer wall diameter was 0.38 mm, and transmissions of >60% at 320 nm[72] and >95% at wavelengths above 360 nm were observed; the samples were placed in a temperature-controlled recirculating bath (0−3 °C). Electronic spectra were obtained at ambient temperature on a Perkin−Elmer model Lambda 19 UV−Vis/near-IR spectrometer, using 1-cm quartz cells retrofitted with a Kontes Teflon stopcock assembly to ensure the integrity of air-sensitive compounds.

2.1.3. Syntheses. The syntheses of *cis*-1,8-bis(pyridin-3-oxy)oct-4-ene-2,6-diyne (bpod, **1**), as well as the $[Cu(bpod)_2]PF_6$ (**2**) and $[Cu(bpod)_2](NO_3)_2$ (**3**) analogues, have been reported elsewhere.[35] The corresponding $Zn(bpod)_2(CH_3COO)_2$ compound (**4**) was prepared as follows: A 50-mL round-bottom flask was charged with 41 mg (0.19 mmol) of $Zn(CH_3COO)_2$ and dissolved in 5 mL of reagent-grade methanol. Subsequently, 114 mg (0.39 mmol) of **1** was dissolved in 5 mL of methanol and added to the zinc acetate solution. The solution was allowed to stir overnight as the desired complex was formed. To this mixture, 20 mL of diethyl ether was added and the solution cooled to 0 °C for 24 h, which produced a white solid. Yield: 67.5 mg (45%). ^{1}H NMR (400 MHz, CD$_3$CN) δ (ppm): 0.92 (s, 6H, 2CH$_3$), 4.92 (s, 8H), 5.97 (s, 4H), 7.36−7.43 (m, 8H), 8.23 (d, 4H), 8.34 (d, 4H). ^{13}C NMR (CD$_3$CN): 22.75 (CH$_3$), 57.56 (OCH$_2$), 85.28 (Cquat), 92.10 (Cquat), 120.86 (CH), 124.68 (CH), 125.69 (CH), 138.78 (CH), 143.52 (CH), 155.0 (Cquat), 179.69 (Cquat). ESI-MS *m/z*: 704 (M$^+$-CH$_3$COO), 645, 473, 414, 353, 291. Anal. Calcd for C$_{40}$H$_{34}$N$_4$O$_8$Zn: C, 62.88; H, 4.49; N, 7.33. Found: C, 63.05; H, 4.16; N, 7.62.

The compound *trans*-1,8-bis(pyridin-3-oxy)oct-4-ene-2,6-diyne (*t*-bpod, **1a**) was prepared using a literature procedure.[41] The reaction of 3-prop-2-ynyloxy-pyridine[73] with *trans*-dichloroethylene, in the presence of Pd(0), CuI, and *n*-BuNH$_2$ in benzene, led to the formation of desired product in 45% yield. ^{1}H NMR (400 MHz, CDCl$_3$) δ (ppm): 4.87 (s, 4H, OCH$_2$), 6.00 (s, 2H, CH), 7.25 (m, 4H), 8.27 (d, 2H), 8.36 (s, 2H). ^{13}C NMR (CDCl$_3$) δ (ppm): 56.68 (OCH$_2$), 85.49 (Cquat), 88.51 (Cquat), 121.08 (CH), 121.63 (CH), 123.15 (CH), 138.26 (CH), 142.89 (CH), 155.56 (Cquat). HRMS (EI), *m/z*: 290.1067 [HRMS Calcd for C$_{18}$H$_{14}$N$_2$O$_2$: 290.1055].

2.1.4. Photolysis of bpod (1). In a sealed J-Young tube, 20 mg (0.07 mmol) of **1** was dissolved in dry, degassed CD$_3$CN and a 10-fold excess of 1,4-cyclohexadiene was added to achieve a total volume of 700 μL. The solution was photolyzed with λ ≥ 395 nm in a temperature-controlled bath (0−3 °C) for 72 h, after which time no precipitate formed, nor was any reaction detected by NMR. The experiment was repeated at 320 and 345 nm and the same result was obtained. On a preparative scale, in a sealed (Kontes) quartz tube, 35 mg (0.12 mmol) of **1** was dissolved in dry, degassed CH$_3$CN (8 mL). To this solution, 22 mL (287 mmol) of dry, degassed 2-propanol was added as a H-atom donor (9.5 M, >2300-fold excess). The resulting concentration of **1** in solution was 4 mM. After photolysis for 72 h, the solvent was removed in vacuo and the remaining yellow oil was redissolved in CD$_3$CN. The ^{1}H NMR and ^{13}C NMR spectra confirmed the identity of the yellow oil as starting material **1**, indicating that, even with a high H-atom donor concentration, no reactivity is observed.

2.1.5. Photolysis of $[Cu(bpod)_2]PF_6$ (2). Under anaerobic conditions, a Schlenk tube was charged with 20 mg (0.03 mmol) of **2** and dissolved in ∼20 mL of dry, degassed (five freeze−pump−thaw cycles) CH$_3$CN. To this solution, either a 10-fold excess of degassed 1,4-cyclohexadiene or >5000-fold excess of 2-propanol was added as a H-atom donor. In both cases, the final concentration of **2** in solution was 1 mM. These solutions were photolyzed with λ ≥ 395 nm within a temperature-controlled bath (0−3 °C) for 4 h (2-propanol) to 12 h

(68) Tullius, T. D.; Dombroski, B. A.; Churchill, M. E. A.; Kam, L. In *Methods in Enzymology*, Vol. 155; Wu, R., Ed.; Academic Press: San Diego, CA, 1987; pp 537−558.
(69) Shimizu, M.; Inoue, H.; Ohtsuka, E. *Biochemistry* **1994**, *33*, 606−613.
(70) Mestre, B.; Pratviel, G.; Meunier, B. *Bioconjugate Chem.* **1995**, *6*, 466−472.
(71) Gravert, D. J.; Griffin, J. H. *Inorg. Chem.* **1996**, *35*, 4837−4847.

(72) Murov, S. L. In *Handbook of Photochemistry*; 2nd ed.; Hug, G. L., Carmichael, I., Eds.; Marcel Dekker: New York, 1993; p 420.
(73) Brandman, H. A.; Freudewald, J. E.; Manowitz, M.; Nikawitz, E. J.; Sharpell, F. H., Jr. Iodopropargyl Pyridyl and Picolinyl Ethers and Thioethers as Paint Fungicides. U.S. Patent 4,170,704, October 9, 1979.

(1,4-cyclohexadiene), depending upon the concentration of H-atom donor. Upon photolysis, the solutions change to a brown color, and a precipitate begins to form within 1 h. To isolate the photoproduct, larger-scale photolyses were performed (~275 mg) using the same ratios of H-atom donor. Upon completion of the photolyses, the solutions were concentrated, stirred with a 1:3 mixture of degassed ether: CH_3CN to precipitate the product, and filtered anaerobically. The solid was subsequently washed with ether and dried in vacuo to yield ~135 mg (47%) of solid metal-containing photoproduct. ^{1}H NMR and ^{13}C NMR spectra of the solid were obtained in degassed CD_3CN and showed exclusive formation of two Bergman-cyclized ligands bound to Cu(I). The NMR spectrum of this species matches that of the thermally cyclized product previously reported very well.[35] ^{1}H NMR (400 MHz, DMSO-d_6) δ (ppm): 5.40 (s, 8H, OCH$_2$Ph), 7.40–7.45 (m, 8H), 7.56–7.59 (m, 4H), 7.69–7.71 (m, 4H), 8.39 (d, 4H), 8.54 (d, 4H). ^{13}C NMR (DMSO-d_6) δ (ppm): 68.9 (OCH$_2$Ph), 122.9 (CH), 125.67 (CH), 129.9 (CH, benzene), 130.38 (CH, benzene), 136.37 (Cquat, benzene), 139.6 (CH), 143.54 (CH), 155.99 (Cquat). ESI-MS m/z: 649.0, 647.2; ^{63,65}Cu [M$^+$ Calcd for C$_{36}$H$_{32}$N$_4$O$_4$Cu: 649.2/647.2], 357.1, 355.1, 293.2.

To analyze the filtrate, the solvent was removed under vacuum, and repeated washings of the viscous brown oil with ether gave a light-brown solid. The solid was subsequently dissolved in degassed CH_3CN and filtered. Solvent was then removed from the filtrate to yield ~90 mg of solid material. The ^{1}H and ^{13}C NMR spectra[35] confirmed the identity of the solid as unreacted starting material (38%–40% initial mass of **2**).

2.1.6. Stoichiometric Analysis of [Cu(bpod)$_2$]PF$_6$ Photoproduct. The solid inorganic photoproduct (~90 mg) was dissolved in ~25 mL of DMF. A 10-fold excess of aqueous Na$_2$EDTA solution was added to sequester the metal, and the mixture was allowed to be stirred gently at 0 °C for 12 h. The precipitate was filtered and the uncomplexed organic material was extracted with dichloromethane. The organic layer was then washed with water, using a separatory funnel, and dried over anhydrous Na$_2$SO$_4$. The resulting brown oil was purified by flash chromatography (20% MeOH/CH$_2$Cl$_2$, R_f = 0.47) and had a yield of 87% (based on 2 mol of ligand per mole of reacted complex) of the dark-yellow Bergman-cyclized ligand. ^{1}H NMR (400 MHz, CDCl$_3$) δ (ppm): 5.24 (s, 4H, OCH$_2$Ph), 7.24 (m, 4H), 7.41 (m, 2H), 7.52 (m, 2H), 8.20 (d, 2H), 8.39 (d, 2H). ^{13}C NMR (CDCl$_3$) δ (ppm): 68.7 (OCH$_2$), 121.24 (CH), 124.35 (CH), 129.24 (CH, benzene), 129.64 (CH, benzene), 134.75 (Cquat, benzene), 138.45 (CH), 142.88 (CH), 155.04 (Cquat). FAB-MS, m/z: 293 (M$^+$ + H), 198. HR-MS (EI), m/z: 292.1208 [HR-MS Calcd for C$_{18}$H$_{16}$N$_2$O$_2$: 292.1214].

2.1.7. Photolysis of [Cu(bpod)$_2$](NO$_3$)$_2$ (3). The same anaerobic procedure used for the photolysis of Cu(bpod)$_2$PF$_6$ was employed for photoreaction of **3** in solution. Briefly, a degassed solution of **3** (200 mg, 0.30 mmol, 1 mM) containing a 10-fold excess of 1,4-cyclohexadiene was photolyzed at 3 °C for 12 h with $\lambda \geq$ 395 nm. The green solution changed to a yellow–brown color after only 4 h, indicating reactivity of the complex in solution. The solution was concentrated and, upon addition of ether, a dark-brown–green precipitate formed. The solid was filtered and washed with ether (96 mg, 48%). Because of the paramagnetism of divalent copper, a cyclized product could not be straightforwardly confirmed by NMR; thus, the metal was extracted using EDTA and the organic products were subsequently analyzed as described for **2** (vide supra). The isolated yield of cyclized ligand product, based on 2 mol of ligand per mole of reacted complex, was 36 mg (81%). ^{1}H NMR (400 MHz, CDCl$_3$) δ (ppm): 5.24 (s, 4H, OCH$_2$Ph), 7.24 (m, 4H), 7.41 (m, 2H), 7.52 (m, 2H), 8.21 (d, 2H), 8.39 (d, 2H). ^{13}C NMR (CDCl$_3$) δ (ppm): 68.72 (OCH$_2$), 121.24 (CH), 124.31 (CH), 129.24 (CH, benzene), 129.66 (CH, benzene), 134.75 (Cquat, benzene), 138.45 (CH), 142.88 (CH), 155.04 (Cquat). FAB-MS, m/z: 293 (M$^+$ + H), 198. HR-MS (EI), m/z: 292.1210 [HR-MS Calcd for C$_{18}$H$_{16}$N$_2$O$_2$: 292.1214].

2.1.8. Photolysis of Zn(bpod)$_2$(CH$_3$COO)$_2$ (4). In a J-Young NMR tube, 31 mg (0.04 mmol) of **4** was dissolved in dry, degassed CD$_3$CN. To this solution, 37 μL (0.39 mmol) of 1,4-cyclohexadiene was added to achieve a final volume of 800 μL (51.3 mM **4**). The reaction mixture was photolyzed at 0 °C for 24 h with $\lambda \geq$ 395 nm, and the progress of the reaction was monitored by ^{1}H NMR. No change in the solution color or composition was detected, and the ^{1}H NMR spectrum of the reaction mixture remained unchanged. The experiment was repeated with $\lambda \geq$ 320 and 345 nm (using quartz and Pyrex cells, respectively) and no reactivity was observed. Compound **4** was also photolyzed under the same conditions, except for the presence of either excess Cu(NO$_3$)$_2$ or Cu(CH$_3$CN)$_4$PF$_6$ (~5-fold excess). Isolation of the organic material by demetalation with EDTA as described previously and subsequent NMR analyses revealed the presence of only the starting material.

2.1.9. Triplet-Sensitized Photolyses of 4. Triplet-sensitized photolyses of **4**, using acetophenone, were performed both on the analytical (J-Young tube) and preparative scales, using 1:9.1 molar ratios of **4**:1,4-cyclohexadiene, with molar acetophenone ratios in the range of 0.13–1.09. In each case, the progress of the photoreaction was monitored by ^{1}H NMR. To fully characterize the reaction products, 248 mg of **4** (0.33 mmol) was dissolved in dry and degassed CH$_3$CN, and 1,4-cyclohexadiene (0.28 mL, 3.0 mmol) and acetophenone (0.35 mmol) were added. The resulting reaction mixture yields a concentration of 16.3 mM for **4** and a sensitizer concentration of 17.5 mM (A_{345} = 2.4, ϵ_{345} = 139 M^{-1} cm^{-1}). Photolysis was conducted at 0 °C for 25 h with $\lambda \geq$ 395 nm. New ^{1}H NMR resonances at 4.94 and 6.06 ppm were observed after 6.5 h. In addition, the ^{13}C NMR spectrum revealed new alkyne resonances, at 85.46 and 88.51 ppm. To allow completion of the reaction, photolysis was continued for 6 days; however, maximum conversion was observed after 72 h (40%). After photolysis, the solvent was removed and the solid obtained was washed with ether. The crude reaction material was dissolved in 20 mL of DMF and treated with a 10-fold molar excess of Na$_2$EDTA and stirred for 10 h at 0 °C. The resulting precipitate was filtered off and the organic material was extracted with CH$_2$Cl$_2$ and washed with excess H$_2$O. After metal extraction, the ^{1}H NMR spectrum of the reaction mixture shows the presence of new features at 4.94 and 6.00 ppm. The ^{13}C NMR spectrum revealed the presence of two new alkyne resonances, at 85.46 and 88.51 ppm, as well as aromatic features, at 121.06, 121.60, and 142.88 ppm. The new ^{1}H and ^{13}C NMR signals match those of the independently synthesized, authentic *t*-bpod, **1a** (vide supra). Other than unreacted starting material, no additional species were detected in solution.

2.1.10. Electrochemistry. All measurements were made using dried CH$_3$CN (distilled) or DMF (sieves) with tetramethylammonium hexafluorophosphate (TMAPF$_6$, Aldrich) as the supporting electrolyte, which was stored in a vacuum oven at 80 °C to remove traces of water. Electrodes were fabricated from a 3-mm-diameter glassy carbon rod (Grade GC-20; Tokai Electrode Manufacturing Co., Tokyo, Japan) and press-fitted into a Teflon shroud to provide a planar, circular electrode with an area of 0.071 cm^2. Before use, the electrode was cleaned with an aqueous suspension of 0.05-μm alumina (Buehler) on a Master-Tex polishing pad (Buehler). For all experiments, the reference electrode was a saturated cadmium amalgam in contact with DMF saturated with both cadmium chloride and sodium chloride. This electrode has a potential of −0.76 V, versus the aqueous saturated calomel electrode (SCE), at 25 °C.[74,75] All quoted potentials have been converted to the SCE scale, and $E_{1/2}$ values were calculated from an average of E_{pa} and E_{pc}. Cyclic voltammograms were obtained in cells previously described,[76] with the aid of a Princeton Applied Research Corporation (PARC) model 175 universal programmer in combination with a PARC model 173 potentiostat–galvanostat and were recorded on a Yokogawa model 3023 $X–Y$ recorder.

(74) Marple, L. W. *Anal. Chem.* **1967**, *39*, 844–846.
(75) Manning, C. W.; Purdy, W. C. *Anal. Chim. Acta* **1970**, *51*, 124–126.
(76) Vieira, K. L.; Peters, D. G. *J. Electroanal. Chem.* **1985**, *196*, 93104.

2.1.11. Photochemical Quantum Yield Determination. Quantum yield measurements were performed via photolysis at 366 nm with a 1000-W HgXe source, utilizing a series of long- (295, 345, 360 nm) and short-wavelength-pass filters (450 nm), as well as a 366 nm notch filter. Freshly purified **1** (33 mg, 1.14×10^{-4} mol) was pumped into the drybox and dissolved into 2.0 mL of dry degassed CD_3CN. To the resulting solution, a solution of 21.4 mg (5.74×10^{-5} mol) $Cu(CH_3CN)_4PF_6$ in 1.0 mL CH_3CN-d_3 was added dropwise. A 460 μL aliquot was then transferred to a J-Young tube and 340 μL (504 molar eq) of dry, degassed 2-propanol-d_8 was added. The resulting solution (11.0 mM **2** in a total volume of 800 μL) was then photolyzed in the J-Young tube and changes in the concentration of **2** were monitored by integration of the olefin resonance at 5.97 ppm in the ^{1}H NMR spectrum, relative to the residual CH_3CN proton resonance. Actinometry measurements were performed using the ferrioxalate method,[72] using 800 μL sample volumes in sealed J-Young NMR tubes. To reduce the error in the actinometry, a total of 15 measurements were made across three groups of five samples at various times throughout the photolysis.

2.1.12. DNA Binding Constant Evaluation. The binding of **3** to calf thymus DNA (Sigma) was determined by a Scatchard analysis via displacement and competitive inhibition of ethidium bromide (EB) binding.[77−79] Specifically, the association constant for **3** was determined by monitoring the fluorescence intensity of EB upon titration of DNA solutions containing varying concentrations of **3** with increasing concentrations of EB. The amount of bound EB (c_b) was calculated using eq 1:[78]

$$c_b = \frac{I_t - I_0}{(V - 1)k} \tag{1}$$

where I_0 is the fluorescence intensity of free EB, I_t the total fluorescence intensity when DNA is present, k the slope of a plot of I_0 vs C_0 (the concentration of EB added), and V the fluorescence ratio of the bound EB to free EB. The concentration of free EB and the ratio of bound EB to the total nucleotide concentration (r_{eb}) was then calculated. From these data, Scatchard plots were constructed using a competitive inhibition model (eq 2):[77,79]

$$\frac{r_{eb}}{c_f} = (n - r_{eb})\left[\frac{K_{eb}}{(1 + K_m c_m)}\right] \tag{2}$$

where K_m and c_m are the association constant and concentration of bound competitor, respectively, n is the number of binding sites, and c_f is the concentration of free EB. Because $K_{obs} = [K_{eb}/(1 + K_m c_m)]$, the association constant for **3** (K_m) was determined from a plot of K_{eb}/K_{obs} vs c_m (eq 3).[79]

$$\frac{K_{eb}}{K_{obs}} = K_m c_m + 1 \tag{3}$$

Concentration ratios of bound EB to free EB were determined by monitoring the fluorescence intensity of EB at $\lambda_{em} = 600$ nm upon $\lambda_{ex} = 510$ nm at 25 °C in a 10 mM tris-acetate buffer at pH 7.6. The concentrations of **3** and EB were varied from 0 to 40 μM and from 4 to 12 μM, respectively, with a corresponding nucleotide concentration of 36 μM, which was determined by the optical density at 260 nm ($\epsilon_{260} = 6600$ M^{-1} cm^{-1} per nucleotide).[80] Samples were incubated for 10 h at 4 °C and, subsequently, 1 h at 25 °C prior to spectral analyses. Control experiments revealed that neither **3** nor $CuCl_2$ have an effect on the fluorescence intensity of free EB. Similarly, $CuCl_2$ does not influence the fluorescence intensity of DNA-bound EB.

2.2. DNA Photocleavage Assays. 2.2.1. Agarose Gel Electrophoresis. Bacterial plasmid pUC19 DNA was obtained from New England Biolabs and used immediately as received. Quantitation of DNA was conducted using established procedures[81] and yielded 250 μg of pUC19 (MW = 1.70×10^6 g/mol, 2686 base pairs (bp)). The plasmid DNA was digested to linear (Form III) DNA by incubating a mixture of 3 μL of Hind III buffer (10×) and 1.5 μL of Hind III enzyme (20 000 units/mL, New England Biolabs), 6.6 μL of pUC19, and 18.9 μL of deionized water for 5 h at 37 °C.

Thermal and photochemical cleavage reactions were performed under deoxygenated conditions in airtight Pyrex conical vials with 50 μM bp of pUC19 in 10 mM tris-acetate pH 7.6 buffer at $\lambda \geq 395$ nm, $t = 8$ h, $T = 20$ °C. All samples were quenched using liquid nitrogen after photolysis, and samples were subsequently stored at −20 °C. The concentration of compounds **2** and **3** ranged from 500 to 12.5 μM in a total volume of 100 μL. The samples for compound **3** were prepared and degassed individually by five freeze−pump−thaw cycles in airtight Pyrex conical vials. Compound **2** was handled under a nitrogen atmosphere in an inert-atmosphere box, and all samples were prepared using degassed 10 mM tris-acetate buffer at pH 7.6. Reaction samples (7 μL) were run on a on a 1% nondenaturing agarose gel (SeaKem Gold agarose, FMC BioProducts Seakem and Genetic Technology Grade) prepared with 1× TAE buffer (60 V, 3 h) and stained with EB (10 mg/mL).

As control experiments, 50 μM DNA was photolyzed alone at $\lambda \geq 395$ nm, $T = 20$ °C (8 h), and complexes **2** and **3** (25 μM) were incubated for 12 h with 50 μM bp plasmid DNA in darkness under aerobic and anaerobic conditions (10 mM tris-acetate buffer, pH 7.6, 200 μL). In addition, inhibitor studies were also conducted according to a literature procedure[82] with 0.5 M ethanol and 100 μg/mL superoxide dismutase (SOD). For the SOD inhibition studies,[82] 1 mg of protein was dissolved in 300 μL of 10 mM tris-acetate buffer (pH 7.6).[83] Aliquots of the samples (7 μL) were stained with EB (10 mg/mL) and analyzed on a 2% nondenaturing agarose gel (SeaKem Gold agarose, FMC BioProducts Seakem and Genetic Technology Grade) prepared with 1× TAE buffer (60 V, 3 h).

2.2.2. Radiolabeling/Non-Denaturing Polyacrylamide Gel Electrophoresis. Synthetic oligonucleotides were purchased from the Lineberger Comprehensive Cancer Center Nucleic Acids Core Facility and purified by gel electrophoresis on a 20% polyacrylamide gel with 7 M urea (Mallinckrodt).[84] All experiments containing DNA (except HPLC experiments) were performed using a 25-bp oligonucleotide with the following sequence (^{32}P-labeled strand): d[5′-(ATG GCG TAA TCA TGG TCA TAG CTG T)-3′]. Water was purified with a MilliQ purification system (Millipore). Buffer salts were purchased from Mallinckrodt. Gel electrophoresis reagents such as acrylamide, agarose, and 10× TBE buffer (0.89 M tris, 0.89 M boric acid, 20 mM EDTA, pH 8.3) were purchased from BioRad.

Solution concentrations of metal complex or DNA were determined by spectrophotometry ($\epsilon_{395} = 167$ M^{-1} cm^{-1} for **3**), using a Hewlett−Packard model HP 8452 diode-array spectrophotometer. Oligonucleotide strand concentrations were determined by absorbance at 260 nm with a calculated extinction coefficient from the nearest-neighbor equation.[85]

Single-stranded oligonucleotide was 5′-radiolabeled using γ^{32}P-ATP (New England Nuclear). A 25 μL solution containing 1 μL of single-stranded oligonucleotide (5 μM), 5 μL of forward reaction buffer (5×),

(77) Scatchard, G. *Ann. N. Y. Acad. Sci.* **1949**, *51*, 660−672.
(78) Le-Pecq, J. B.; Paoletti, C. J. *J. Mol. Biol.* **1967**, *27*, 87−106.
(79) Howe-Grant, M.; Wu, K. C.; Bauer, W. R.; Lippard, S. J. *Biochemistry* **1976**, *15*, 4339−4346.
(80) Reichmann, M. E.; Rice, S. A.; Thomas, C. A.; Dotty, P. *J. Am. Chem. Soc.* **1954**, *76*, 3047−3053.

(81) Ausubel, F. M.; Brent, R.; Kingston, R. E.; Moore, D. D.; Seidman, J. G.; Smith, J. A.; Struhl, K. In *Current Protocols in Molecular Biology*; 2nd ed.; John Wiley & Sons: New York, 1994−1997.
(82) Speetjens, J. K.; Parand, A.; Crowder, M. W.; Vincent, J. B.; Woski, S. A. *Polyhedron* **1999**, *18*, 2617−2624.
(83) SOD was purchased from Sigma and contained 3800 units per milligram of solid. One unit corresponds to the amount of catalytic enzyme that inhibits the autoxidation of pyrogallol by 50% at pH 8.2 and 25 °C.
(84) Sambrook, J.; Fritsch, E. F.; Maniatis, T. In *Molecular Cloning: A Laboratory Manual*; 2nd ed.; Cold Spring Harbor Laboratory Press: Plainview, NY, 1989.
(85) Fasman, G. D. *Handbook of Biochemistry and Molecular Biology, Section B*; CRC Press: Cleveland, OH, 1976; Vol. I.

Scheme 1. Synthesis of *t*-bpod Ligand (**1a**)
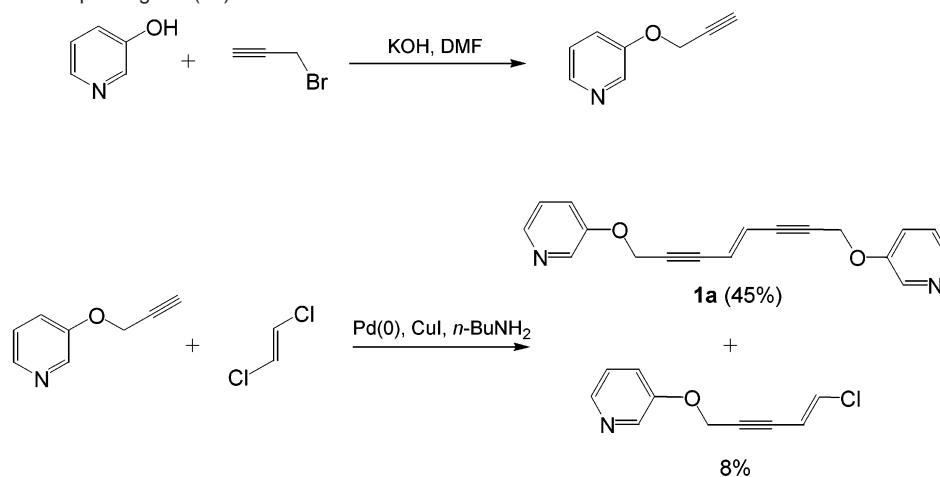
1 μL of T4 polynucleotide kinase (Life Technologies), and 17 μL MilliQ H$_2$O was heated in a water bath at 37 °C for 20 min. The T4 polynucleotide kinase was deactivated by heating the reaction solution at 65 °C for 10 min. The ^{32}P-labeled oligonucleotide (diluted to 50 μL) was then purified on a MicroSpin model G-50 column (Amersham Pharmacia Biotech). The resulting ^{32}P-labeled oligonucleotide was ethanol-precipitated and resuspended in MilliQ water ($\sim$400 K cts/5 μL).[84] Oligonucleotides labeled on the 3′ end were similarly generated using published procedures.[84]

Radiolabeled double-stranded oligonucleotide solutions were prepared by mixing a 1:1.2 ratio of 20 μM stock solutions of unlabeled oligonucleotide and complementary oligonucleotide in 20 mM sodium phosphate buffer (pH 7). ^{32}P-labeled oligonucleotide (5 μL, 400 cts) was added to each 20 μL of reaction solution. The resulting mixture was heated to 90 °C for 5 min and cooled to room temperature over 2 h to anneal the strands. Formation of the hybridized duplex was confirmed using native gel electrophoresis.

Stock solutions of **3** ($\sim$25 mM) were prepared in DMF (Fisher) and kept at 4 °C until being diluted to 200 μM immediately before addition to solutions of ^{32}P-labeled oligonucleotide. Hybridized ^{32}P-labeled oligonucleotide (20 μL) was combined with the appropriate amounts of MilliQ H$_2$O and 1.8 mM **3** to yield a total reaction solution (40 μL) consisting of 10 mM sodium phosphate (pH 7), 10 μM oligonucleotide, and varying concentrations (0, 90, 180, 270 μM) of **3**. In a polyspring insert tube (National Scientific Company), the reaction solution was photolyzed for 8 h with a 300-W Hg lamp (Oriel) and a monochromator set to 368 nm (60% transmission, 40 nm full width at half-maximum (fwhm)). Following photolysis, the reactions were quenched with 2 μL of EDTA (1 mM) and ethanol-precipitated with sodium acetate, as described elsewhere.[84] Select samples were treated with piperidine prior to denaturing gel electrophoresis.[84] Control reactions were also performed with single-stranded ^{32}P-labeled oligonucleotide in place of the double-stranded ^{32}P-labeled oligonucleotide and CuCl$_2$ in place of **3**.

2.2.3. Hydroxyl Radical Reaction. Fe(EDTA)$^{2-}$/H$_2$O$_2$ reactions with oligonucleotides were performed according to published procedures.[68] Briefly, equal amounts of a freshly prepared solution of 0.4 mM ferrous ammonium sulfate (Aldrich) and 0.8 mM EDTA solution were combined in an Eppendorf tube. The resulting 0.4 mM Fe(EDTA)$^{2-}$ solution was diluted to 80 μM. In a clean Eppendorf tube, 5 μL of ascorbate (8 mM, Sigma), 5 μL of Fe(EDTA)$^{2-}$ (80 μM), and 5 μL of H$_2$O$_2$ (0.024%, Mallinckrodt) were combined. Subsequently, 20 μL of radiolabeled oligonucleotide (20 μM) was added to the mixture. The reaction solution was allowed to react for 12 min at room temperature, quenched with 10 μL of thiourea (0.1 M, Mallinckrodt) and 1 μL of EDTA (0.2 M, Mallinckrodt), and ethanol-precipitated. Selected reactions were treated with piperidine prior to denaturing gel eletrophoresis.[84]

2.2.4. Fragment Modification. Procedures for modification of oligonucleotide fragments were conducted in a manner similar to previously published methods.[86] Briefly, samples to be treated with sodium borohydride (NaBH$_4$) were pelleted by centrifugation at 16 000g for 20 min after the cleavage reaction, quenching, and ethanol precipitation. The dried pellet was resuspended in 40 μL of NaBH$_4$ (0.2 M, Aldrich) and allowed to react for 15 min at room temperature. The reaction was quenched with 8 μL of acetic acid and ethanol-precipitated again. These samples were not subjected to piperidine treatment.

2.2.5. Denaturing Polyacrylamide Gel Electrophoresis. All samples were pelleted by centrifugation at 16 000g for 20 min and resuspended in 12 μL of gel-loading dye solution (80% formamide, 0.5$\times$ TBE buffer, and orange G dye), and heated at 90 °C for 5 min. Each sample (6 μL) was loaded into a well of 20% denaturing polyacrylamide gel containing 7 M urea and run at 65 W for 5 h. The gel was then transferred to a phosphor imaging screen, exposed overnight, and scanned on a Storm 840 System PhosphorImager (Molecular Dynamics).

3. Results

3.1. Syntheses. The synthesis of *cis*-1,8-bis(pyridin-3-oxy)-oct-4-ene-2,6-diyne (bpod, **1**) can be accessed via the Sonashigura cross-coupling approach, using more than one route, as have been previously described.[35,41] The *trans*-1,8-bis(pyridin-3-oxy)oct-4-ene-2,6-diyne (*t*-bpod, **1a**) derivative was prepared using a similar method, with substitution of *trans*-1,2-dichloroethylene for the cis-isomer (Scheme 1). The corresponding [Cu(bpod)$_2$]PF$_6$ (**2**) and [Cu(bpod)$_2$](NO$_3$)$_2$ (**3**) complexes are straightforwardly prepared using 2.1:1 bpod:Cu stoichiometry.[35] The analogous Zn(bpod)$_2$(CH$_3$COO)$_2$ compound (**4**) was similarly prepared by dissolving Zn(CH$_3$COO)$_2$ in MeOH with a subsequent addition of 2.1 equiv of ligand **1**. The solution was allowed to be stirred overnight and, upon addition of ether, was then cooled to 0 °C for 24 h to produce the off-white solid in 45% isolated yield (Scheme 2).

3.2. Electrochemistry. Reduction potentials for compounds **1**−**3** are given in Table 1. In general, **1**, in both the uncomplexed and complexed states, exhibits two irreversible waves between E_p values of −1.75 and −1.93 V (vs SCE), corresponding to reductions of the alkyne units.[43,87] Irreversible, ligand-based one-electron oxidation waves are also observed at +1.94 and +2.15 V (vs SCE) for **1** and **3**, respectively, whereas for **2**, this

(86) Breiner, K. M.; Daugherty, M. A.; Oas, T. G.; Thorp, H. H. *J. Am. Chem. Soc.* **1995**, *117*, 11673−11679.
(87) Martin, R. E.; Gubler, U.; Cornil, J.; Balakina, M.; Boudon, C.; Bosshard, C.; Gisselbrecht, J.-P.; Diederich, F.; Gunter, P.; Gross, M.; Bredas, J.-L. *Chem.—Eur. J.* **2000**, *6*, 3622−3635.

Scheme 2. Synthesis of Zn(bpod)$_2$(CH$_3$COO)$_2$ (**4**)
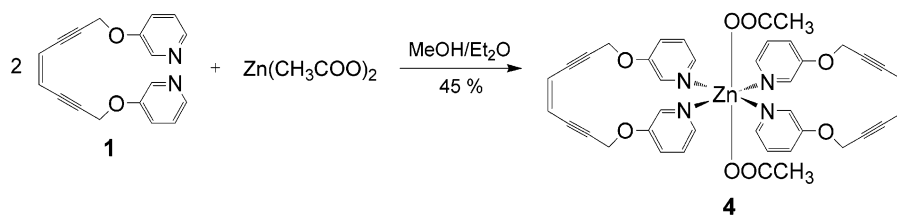
Table 1. Electrochemical Data for **1**−**3** (vs SCE) at 25 °C

compound	$E_{1/2}$ Cu, 2+/+ (V)	E_p Cu, +/0 (V)	E_p bpod (V)		
			+/0	0/−	−/2−
bpod(**1**)[a]			+1.94(ir)	−1.75(ir)	−1.93(ir)
[Cu(bpod)$_2$]PF$_6$ (**2**)[b]	+0.15	−0.95(ir)		−1.80(ir)	−1.92(ir)
[Cu(bpod)$_2$](NO$_3$)$_2$ (**3**)[a]	+0.38	−0.85(ir)	+2.15(ir)	−1.76(ir)	−1.93(ir)

[a] Redox potentials recorded in CH$_3$CN. [b] Redox potentials recorded in DMF. The uncertainty in the reported potential is ±0.02 V.
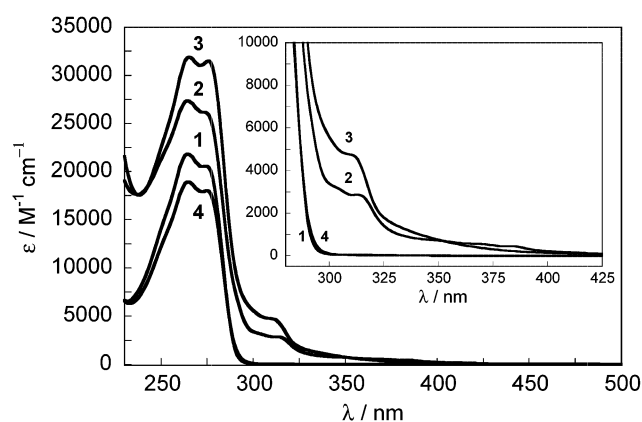
Figure 1. Electronic absorption spectra of **1**−**4** in CH$_3$CN at 25 °C.

Table 2. Electronic Absorption Spectral Data for **1**−**4** Obtained in CH$_3$CN at 25 °C

compound	λ_{max}/nm[a] (ϵ/M^{-1} cm^{-1})
bpod (**1**)	264 (21 800), 276 (20 300)
[Cu(bpod)$_2$]PF$_6$ (**2**)	265 (27 400), 276 (25 900), 315 (2800)
[Cu(bpod)$_2$](NO$_3$)$_2$ (**3**)	265 (31 900), 276 (31 500), 311 (4700)
Zn(bpod)$_2$(CH$_3$COO)$_2$ (**4**)	264 (18 900), 276 (17 900)

[a] The uncertainty in the reported λ_{max} is ±2 nm.

Binding of **1** to redox-active Cu^{2+} results in a marked increase in the extinction of the transitions at 265 nm (ϵ = 31 900 M^{-1} cm^{-1}) and 276 nm (ϵ = 31 500 M^{-1} cm^{-1}), while, to a lower energy, a broad absorption feature is observed at 311 nm (ϵ = 4700 M^{-1} cm^{-1}). To a first approximation, pyridine-to-Cu^{2+} ligand-to-metal charge-transfer (LMCT) transitions can be identified as promotions from the pyridine σ (formally the nonbonding lone pair) and π_1 and π_2 (perpendicular to the ring plane) orbitals[90] to the half-occupied d$_{x^2-y^2}$ orbital centered on the Cu^{2+} cation, as have been described for Cu-imidazole complexes.[91,92] The strongly allowed ring N(σ)-to-Cu(d$_{x^2-y^2}$) LMCT transition occurs at high energy (<300 nm) and is obscured by the prominent ligand-centered transitions. Descent in symmetry due to deviations from a rigorous d$_{x^2-y^2}$ square plane[35] and rotation of the pyridine rings about the metal−ligand bond[35,93] permit mixing of dπ character into the Cu(d$_{x^2-y^2}$) HOMO. This generates pyridine(π)−Cu(HOMO) overlap and thus pyridine(π)-to-Cu LMCT transitions of moderate intensity in the 300−375 nm range[91,92] that are not affected strongly by the enediyne unit.[94]

For the d^{10} Cu$^+$ complex **2** in a pseudo-tetrahedral geometry,[35] the same two strong ligand-centered $\pi-\pi^*$ transitions are observed at 265 nm (ϵ_{265} = 27 400 M^{-1} cm^{-1}) and 276 nm

oxidation process occurs outside the solvent (DMF) window (+1.2 V, vs SCE) and is not detected. These values compare favorably with those obtained for the 1,8-bis(tetrahydropyran-2-yloxy)oct-4-ene-2,6-diyne precursor to **1**, identifying these waves as enediyne-localized redox processes.[88] Two metal-centered redox processes are also observed for **2** and **3**, corresponding to 2+/+ (reversible) and +/0 (irreversible) redox couples. For **2**, the Cu(II)/Cu(I) couple occurs at $E_{1/2}$ = +0.15 V, whereas for **3**, reduction to Cu(I) occurs at a noticeably positive potential ($E_{1/2}$ = +0.38 V), indicating the relative ease of reduction to the Cu(I) state. Not surprisingly, the Cu(I)/Cu(0) redox couple is irreversible and is observed at more-negative potentials (E_p values from −0.85 to −0.95 V, vs SCE).

3.3. Electronic Spectra. Electronic absorption spectra of **1**−**4** at ambient temperature in dry, degassed CH$_3$CN are shown in Figure 1, and the peak maxima are given in Table 2. The uncomplexed enediyne ligand **1** possesses two absorption features, at 264 nm (ϵ = 21 800 M^{-1} cm^{-1}) and 276 nm (ϵ = 20 300 M^{-1} cm^{-1}), that are comprised of primarily 3-alkoxy-pyridine $\pi-\pi^*$ transitions.[89] Complexation of **1** to Lewis-acidic Zn^{2+} produces no shifts in the energies and only a slight decrease in the molar extinction of the transitions at 264 nm (ϵ = 18 900 M^{-1} cm^{-1}) and 276 nm (ϵ = 17 900 M^{-1} cm^{-1}).

(88) Redox potentials for the compound 1,8-bis(tetrahydropyran-2-yloxy)oct-4-ene-2,6-diyne are comparable ($E_{1/2}$ = +2.0, −2.05, −2.25) to the ligand-centered redox potentials reported in Table 2, thereby establishing the redox process as localized on the enediyne portion of the molecule.

(89) Silverstein, R. M.; Bassler, G. C.; Morrill, T. C. *Spectrometric Identification of Organic Compounds*; 4th ed.; John Wiley & Sons: New York, 1981.
(90) Innes, K. K.; Ross, I. G.; Moomaw, W. R. *J. Mol. Spectrosc.* **1988**, *132*, 492−544.
(91) Bernarducci, E.; Schwindinger, W. F.; Hughey, J. L.; Krogh-Jespersen, K.; Schugar, H. J. *J. Am. Chem. Soc.* **1981**, *103*, 1686−1691.
(92) Fawcett, T. G.; Bernarducci, E. E.; Krogh-Jespersen, K.; Schugar, H. J. *J. Am. Chem. Soc.* **1980**, *102*, 2598−2604.
(93) Pradilla, S. J.; Chen, H. W.; Koknat, F. W.; Fackler, J. P., Jr. *Inorg. Chem.* **1979**, *18*, 3519−3522.
(94) We have synthesized[93] and characterized [Cu(OMePy)$_4$](NO$_3$)$_2$ that exhibits ligand-centered $\pi-\pi^*$ absorption between 250 and 300 nm (ϵ = 15 800 M^{-1} cm^{-1}) and LMCT absorption between 300 and 350 nm (ϵ = 1900 M^{-1} cm^{-1}), whereas uncomplexed OMePy absorbs strongly only between 250 and 300 nm (ϵ = 3800 M^{-1} cm^{-1}).

Scheme 3. Photo-Bergman Cyclization of [Cu(bpod)$_2$]$^+$ (**2**) with $\lambda \geq$ 395 nm

Scheme 4. Photo-Bergman Cyclization of [Cu(bpod)$_2$]$^{2+}$ (**3**) with $\lambda \geq$ 395 nm
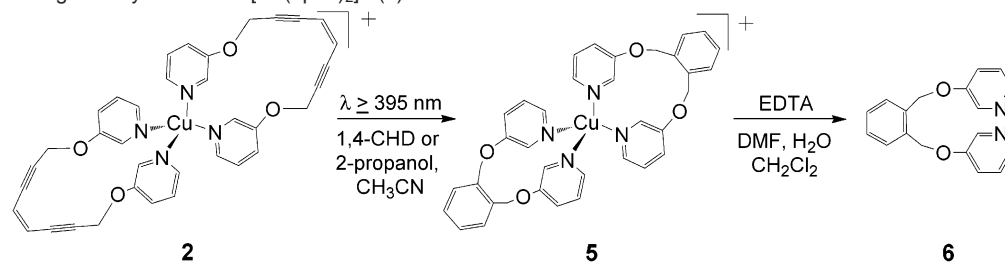
(ϵ_{276} = 25 900 M^{-1} cm^{-1}), along with a distinct Cu$^+$(dπ)-to-pyridine(π^*) MLCT envelope that is observed at 315 nm (ϵ_{315} = 2800 M^{-1} cm^{-1}).[95–102] The pseudo-tetrahedral geometry of the Cu(I) center, combined with free rotation of the pyridine rings, once again permits strong Cu$^+$(dπ)−pyridine(π^*) overlap and thus charge-transfer transitions with π-character. Overall, for both the Cu^{2+} and Cu$^+$ cases, these ligand-centered and charge-transfer (CT) absorption features parallel in energy− and, more coarsely, in intensity−those generally observed for the corresponding tetrakis(*N*-heterocycle) complexes of copper.

3.4. Photochemistry of 1−3. Photochemical reactivities of enediynes **1−3** were studied with $\lambda \geq$ 395 nm. Compound **1** (4 mM) was anaerobically photolyzed for 72 h at 0−3 °C in a constant-temperature bath in the presence of 1,4-cyclohexadiene (CHD) (10-fold excess) or 2-propanol (>2300-fold excess). After photolysis for 72 h, the solvent was removed under vacuum, and the resulting yellow oil analyzed by NMR (^{1}H, ^{13}C). The ^{1}H and ^{13}C NMR spectra confirmed the identity of the yellow oil as starting material, indicating that no reactivity was observed under these reaction conditions.

In contrast, the Cu(I) complex **2** (1 mM) was photolyzed using CHD (10-fold excess) or 2-propanol (> 5000-fold excess) as a H-atom donor in degassed CH$_3$CN under anaerobic conditions. The ^{1}H NMR spectrum indicates a new resonance at 5.40 ppm and a change in the chemical shifts in the aromatic region after 1 h, concurrent with the formation of a brown precipitate. The new resonances located at 5.40 ppm and in the aromatic region became constant after 4 h (2-propanol) and 12 h (CHD) of photolysis, respectively. After the reaction mixture was concentrated, an oily material was isolated and stirred in a mixture of ether and acetonitrile (1:3), to remove the unreacted starting material. The amount of unreacted starting material was confirmed to be 38−40 wt %. Filtration and washing of the brown precipitate with a mixture of ether and CH$_3$CN gave 45%−50% of the solid product. The ^{1}H NMR spectrum of the solid showed a new resonance at 5.40 ppm for the −OCH$_2$Ph unit, as well as two multiplets at 7.57 (4H) and 7.68 (4H) ppm from the disubstituted benzene framework. Furthermore, a ^{13}C NMR spectrum revealed the presence of a disubstituted benzene unit with resonances at 129.90, 130.38, and 136.37 ppm, which
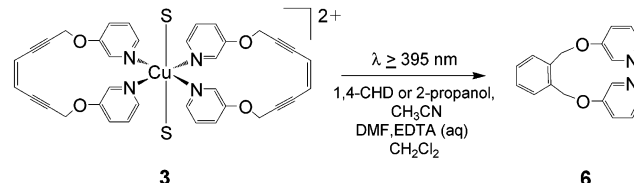
is characteristic of two cyclized enediyne ligands bound to Cu(I) (**5**, Scheme 3). The metal was isolated from the organic transformation product by dissolving the crude solid in a DMF/aqueous EDTA solution. Filtration and subsequent isolation by column chromatography afforded the pure organic photoproduct. The ^{1}H NMR spectrum of the demetalled organic photoproduct exhibited resonances at 5.24 (OCH$_2$Ph), 7.24, 7.41, 7.52, 8.20, and 8.39 ppm that match those of uncomplexed, Bergman-cyclized compound **6** (87% yield).[35] The diamagnetic Cu(I) photoproduct **5** was also fully characterized (^{1}H, ^{13}C NMR, HRMS) and, through comparison to the isolated thermal product previously reported,[35] was determined to possess two Bergman-cyclized ligands bound to Cu(I) (Scheme 3).

Photolysis of [Cu(bpod)$_2$](NO$_3$)$_2$, **3**, changes the color of the bright-green starting solution to yellow−brown after only 4 h. The solution was photolyzed for a total of 12 h; however, unlike the Cu(I) photolysis reaction, no precipitate formed. The solvent from the reaction mixture was removed and, upon the addition of ether, a dark brown−green powder was obtained in 48% yield. The same workup used to isolate the organic photoproduct for **2** was employed to remove the metal and extract the reacted organic ligand. The NMR (^{1}H, ^{13}C) and mass spectral data of the organic photoproduct after demetalation (81% based on two ligands/Cu) are identical to those of the Bergman-cyclized product **6** obtained from photolysis of **2**, as well as from the thermal cyclization of **3** in solution, thereby confirming the photo-Bergman cyclization reactivity of **3** (Scheme 4).

3.5. Photochemistry of 4. Zn(bpod)$_2$(CH$_3$COO)$_2$, **4**, was photolyzed using reaction conditions comparable to those previously discussed. Photolysis of **4** using a 10-fold excess of CHD as a H-atom donor with $\lambda \geq$ 395 nm was conducted at a temperature of 0−3 °C. The reaction mixture was photolyzed for 24 h, and the progress of the reaction monitored by ^{1}H NMR spectroscopy. After 24 h, the ^{1}H NMR spectrum of the reaction mixture remained unchanged and revealed the presence of only starting material, with no indication of decomposition. The same experiment was also conducted with $\lambda \geq$ 320 and 345 nm under identical conditions, and, once again, no reactivity was observed. To determine if free copper could contribute to Bergman cyclization, **4** was photolyzed under the same conditions in the presence of either Cu(NO$_3$)$_2$ or Cu(CH$_3$CN)$_4$PF$_6$ (~5-fold

(95) Kitagawa, S.; Munakata, M.; Higashie, A. *Inorg. Chim. Acta* **1982**, *59*, 219−223.
(96) Ichinaga, A. K.; Kirchhoff, J. R.; McMillin, D. R.; Dietrich-Buchecker, C. O.; Marnot, P. A.; Sauvage, J. P. *Inorg. Chem.* **1987**, *26*, 4290−4292.
(97) Sauvage, J.-P. *Acc. Chem. Res.* **1990**, *23*, 319−327.
(98) Benniston, A. C.; Grossheny, V.; Harriman, A.; Ziessel, R. *Angew. Chem., Int. Ed. Engl.* **1994**, *33*, 1884.
(99) Juris, A.; Ziessel, R. *Inorg. Chim. Acta* **1994**, *225*, 251−254.
(100) Grosshenny, V.; Harriman, A.; Ziessel, R. *Angew. Chem., Int. Ed. Engl.* **1995**, *34*, 1100−1102.
(101) Simon, J. A.; Palke, W. E.; Ford, P. C. *Inorg. Chem.* **1996**, *35*, 6413−6421.
(102) McMillin, D. R.; McNett, K. M. *Chem. Rev.* **1998**, *98*, 1201−1220.

excess). Isolation of the organic material and subsequent NMR analyses revealed the presence of only starting material.

In the absence of direct photochemical reactivity of **4**, a triplet-state sensitizer (acetophenone) was employed to determine if reactivity could be induced via bimolecular energy transfer. Photolysis of complex **4** (16.3 mM) in the presence of CHD (9-fold excess) and acetophenone (17.5 mM) yielded new ^{1}H resonances at 4.94 and 6.06 ppm, as well as a multiplet in the aromatic region after 6.5 h with no evidence of unbound ligand or uncomplexed acetate counterions. The reaction was allowed to continue for six days, but maximum conversion (35−40%) was observed after 72 h. After photolysis, the solvent was removed and the solid obtained was washed with ether. The resulting solid was dissolved in DMF and treated with an aqueous EDTA (excess) solution. Subsequent filtration and extraction of the organic products with CH_2Cl_2 produced a light-yellow oil. The ^{1}H NMR spectrum of the organic reaction mixture exhibited the presence of new resonances at 4.94 and 6.00 ppm, and the ^{13}C NMR spectrum showed the presence of two new alkyne resonances, at 85.46 and 88.51 ppm, as well as aromatic features at 121.06, 121.60, and 142.88 ppm. These features are identical to those of authentic *t*-bpod, **1a**, therefore indicating that the triplet sensitization of **4** leads to ligand isomerization and not Bergman-cyclized product.

3.6. Quantum Yield For Photocyclization. The quantum yield for photocyclization of **2** was performed via photolysis at 366 nm with 1000-W HgXe source utilizing a series of long- and short-pass filters as well as a 366 nm notch filter. From a total of 15 measurements made across three groups of five samples at various times throughout the photolysis, the quantum yield for photocyclization of **2** (ϕ_{366}) was determined to be 4.2 ($\pm$ 0.6) $\times$ 10^{-5}. The absolute magnitude of this value is low and is consistent with the need for photolysis times exceeding 2 h before product is detected.

3.7. DNA Binding. The association constant for **3** with calf thymus DNA was determined by a Scatchard analysis via displacement and competitive inhibition of EB binding at pH 7.6 in 10 mM tris-acetate buffer.[77−79] Binding isotherms (eq 2) converged at a single abssica value (r_{eb} = 0.18), confirming competitive inhibition of EB binding by **3**. These plots, as well as that of K_{eb}/K_{obs} vs c_m (eq 3), yielded excellent linear fits (R^2 > 0.98) and, consequently, an association constant K_m for **3** of 2.6 ($\pm$ 0.2) $\times$ 10^4 M^{-1}. The association constant is significantly decreased, relative to Os(DPPZ)(4,4′-amino-2,2′-bipyridine)$_2^{2+}$ (K_m = 3.1 $\times$ 10^7 M^{-1}),[103] the meso-pyridal porphyrins ($K_m \approx$ 10^5−10^7 M^{-1}),[104] and the Pt/Pd(terpy)(X)$^+$ complexes ($K_m \approx$ 10^5 M^{-1}),[79,105] but is comparable to M(phen)$_y^{x+}$ motifs such as [Cu(phen)$_2$]$^+$ (K_m = 5 $\times$ 10^4 M^{-1}),[106] [Co(phen)$_3$]$^{3+}$ (K_m = 2.6 $\times$ 10^4 M^{-1}),[107] [Co(phen)$_3$]$^{2+}$ (K_m = 1.6 $\times$ 10^4 M^{-1}),[107] [Fe(phen)$_3$]$^{2+}$ (K_m = 7.1 $\times$ 10^3 M^{-1}),[107] [Fe(phen)$_3$]$^{3+}$ (K_m = 1.46 $\times$ 10^4 M^{-1}),[107] and [Ru(phen)$_3$]$^{2+}$ (K_m = 6.2 $\times$ 10^3 M^{-1}).[108] Clearly, the minimal planar π-system of **3** yields an intercalative association constant that is more comparable to those of classical phenanthroline and terpy metal complexes than
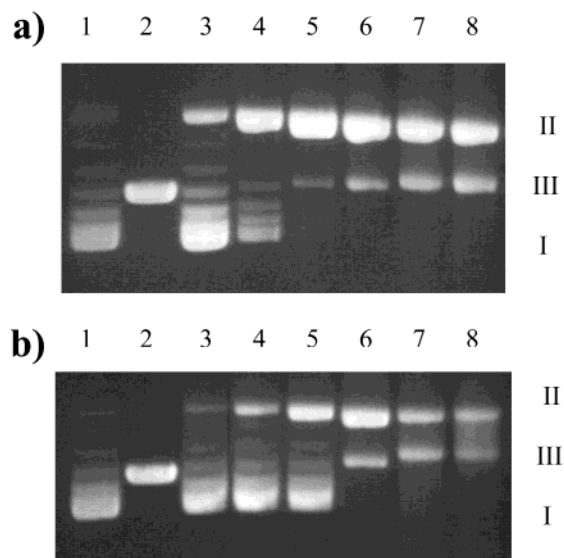
Figure 2. Agarose gel (1%) electrophoretic analysis of the photoinduced cleavage of 50 μM pUC19 plasmid DNA (2686 bp) by **2** and **3** upon $\lambda \geq$ 395 nm photolysis at 20 °C for 8 h. Form I, supercoiled plasmid; Form II, nicked plasmid; Form III, linear plasmid. For panel a, the lanes are identified as follows: 1, DNA (marker); 2, Hind III digest of DNA (marker); 3, DNA; 4, DNA + 12.5 μM **2**; 5, DNA + 50 μM **2**; 6, DNA + 100 μM **2**; 7, DNA + 250 μM **2**; 8, DNA + 500 μM **2**. For panel b, the lanes are identified as follows: 1, DNA (marker); 2, Hind III digest of DNA (marker); 3, DNA; 4, DNA + 10 μM **3**; 5, DNA + 25 μM **3**; 6, DNA + 50 μM **3**; 7, DNA + 250 μM **3**; 8, DNA + 500 μM **3**.

those of the more strongly binding extended aromatic porphyrin or DPPZ-containing metal complexes.

3.8. Plasmid DNA Photocleavage Reactions. Anaerobic photolysis ($\lambda \geq$ 395 nm) of **2** in aqueous solution (10 mM tris-acetate, pH 7.6) in the presence of pUC19 at 20 °C for 8 h (Figure 2a) leads to the generation of nicked plasmid (Form II) at low concentrations (12.5 μM **2**, lane 4). At higher concentrations of **2** (50−500 μM, lanes 5−8), a mixture of linear (Form III) and nicked plasmid is detected, with complete consumption of the supercoiled Form I. Quantitations of the band densities of lanes 5−8 reveal an increasing linear/nicked ratio (0.25−0.68) with increasing concentration of **2**; however, between 250 and 500 μM, the ratio is essentially constant. These results suggest that linear Form III DNA likely is derived from multiple nicking.

Analogous results are obtained upon photolysis of **3** under the same conditions (Figure 2b). At low concentrations of **3** (10−25 μM, lanes 4−5), a mixture of unreacted supercoiled Form I and nicked Form II DNA is observed. At concentrations of **3** from 50 to 500 μM (lanes 6−8), supercoiled Form I DNA is completely consumed and a mixture of linear Form III and nicked Form II DNA remains. Very similar to the cleavage results at higher concentrations of **2**, the ratio of linear/nicked DNA increases only modestly, from 0.7 to 0.98, as the concentration of **3** increases, culminating in essentially a 1:1 ratio of the two forms. Once again, at low concentrations of **3**, the presence of nicked Form II DNA in the absence of linear Form III (lanes 4−5) suggests that a significant contribution of

(103) Maruyama, K.; Mishima, Y.; Minagawa, K.; Motonaka, J. *Anal. Chem.* **2002**, *74*, 3698−3703.
(104) Sari, M. A.; Battioni, J. P.; Dupre, D.; Mansuy, D.; Le Pecq, J. B. *Biochemistry* **1990**, *29*, 4205−4215.
(105) Jennette, K. W.; Lippard, S. J.; Vassiliades, G. A.; Bauer, W. R. *Proc. Natl. Acad. Sci. U.S.A.* **1974**, *71*, 3839−3843.

(106) Veal, J. M.; Rill, R. L. *Biochemistry* **1991**, *30*, 1132−1140.
(107) Carter, M. T.; Rodriguez, M.; Bard, A. J. *J. Am. Chem. Soc.* **1989**, *111*, 8901−8911.
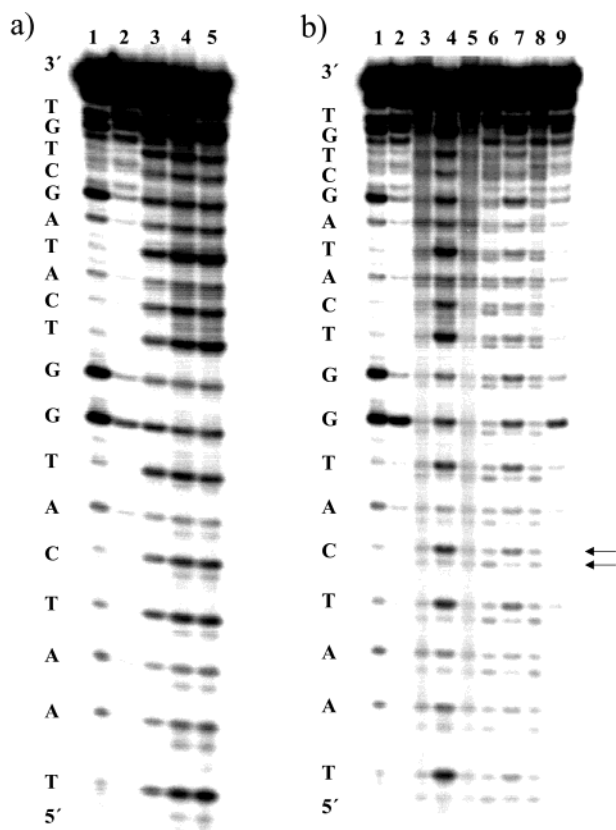(108) Barton, J. K.; Danishefsky, A.; Goldberg, J. *J. Am. Chem. Soc.* **1984**, *106*, 2172−2176.

Figure 3. Polyacrylamide sequencing gels (20%) of the photoinduced (λ = 368 nm, 8 h) cleavage of 5′-radiolabeled ds oligonucleotide d[5′-(ATG GCG TAA TCA TGG TCA TAG CTG T)-3′]. Panel a shows the concentration dependence (0−270 μM **3**) of the cleavage of 10 μM oligonucleotide in 10 mM sodium phosphate, pH 7.0. Lanes are identified as follows: 1, Maxam−Gilbert G lane (cold [DNA] = 5 μM); 2, 10 μM ds oligonucleotide; 3, lane 2 + 90 μM **3**; 4, lane 2 + 180 μM **3**; 5, lane 2 + 270 μM **3**. Panel b depicts the analysis of the oligonucleotide cleavage products by chemical modification (piperidine, NaBH$_4$) and a comparison to the C-4′ H-atom abstraction products from Fe(EDTA)$^{2-}$/H$_2$O$_2$ treatment. Lanes are identified as follows: 1, Maxam−Gilbert G lane (cold [DNA] = 5 μM); 2, 10 μM ds oligonucleotide; 3, lane 2 + 270 μM **3**; 4, lane 3 + piperidine treatment; 5, lane 3 + NaBH$_4$ treatment; 6, lane 2 + Fe(EDTA)$^{2-}$/H$_2$O$_2$; 7, lane 6 + piperidine treatment; 8, lane 6 + NaBH$_4$ treatment; 9, lane 2 + 30 μM CuCl$_2$.

linear DNA likely is derived from multiple nicking. The insensitivity of the DNA degradation patterns upon photolysis of either **2** or **3** in the presence of inhibitors[109] such as superoxide dismutase (SOD) or hydroxy radical scavengers such as ethanol suggests that DNA degradation does not result from residual oxygen-derived radical species.

3.9. 5′-(^{32}P)-Labeled Oligonucleotide DNA Photocleavage Reactions. Anaerobic photolysis of **3**, as a function of concentration (100−300 μM) in the presence of 5′-radiolabeled d[5′-(ATG GCG TAA TCA TGG TCA TAG CTG T)-3′], generates nonspecific cleavage sites distributed systematically along the strand, with the extent of cleavage increasing with increasing concentration of **3** (lanes 3−5, Figure 3a). Closer inspection of the gel reveals a ladder of two bands, indicating the presence of two distinct cleavage products. Treatment of the photoreaction (270 μM **3**, Figure 3b, lane 3) with piperidine yields enhancement of the slower-migrating band, thereby identifying this product as containing 5′-phosphate termini

(109) Parand, A.; Royer, A. C.; Cantrell, T. L.; Weitzel, M.; Memon, N.; Vincent, J. B.; Crowder, M. W. *Inorg. Chim. Acta* **1998**, *268*, 211−219.

(Figure 3b, lane 4).[64,110] Subsequent treatment of the photoreaction products with a reductant such as NaBH$_4$ produces no change in the quantity of either product (lane 5), thus ruling out the 3′-phosphoglycaldehyde product that is derived from C-3′ H-atom abstraction as the faster migrating species.[111] Comparison of the migrations of the photoreaction products from the well-characterized Fe(EDTA)$^{2-}$/H$_2$O$_2$ thermal DNA degradation reaction upon treatment with piperidine and NaBH$_4$ (Figure 3b, lanes 6−8) shows similar behavior, indicating that the faster migrating species is the 3′-phosphoglycolate that is derived from C-4′ activation.[64,86] The absence of a slower-moving band containing a (−3′-furanone−) suggests that the mechanism does not involve abstraction of the 1′ H-atom.[64,86] This result is supported by HPLC analyses of the photoreaction mixtures, which do not show the presence of 5-MF, which is a signature of 1′ H-atom abstraction.[64,86,111] Photolysis experiments with 3′-(^{32}P)-labeled oligonucleotide resulted in a single band corresponding to the phosphate termini. A second band due to the 5′-aldehyde product that is derived from activation at the 5′ position was not detected.[64,86] Combined, these results identify the origin of DNA degradation by photolysis of **3** as C-4′ H-atom abstraction and not base-centered redox chemistry.

4. Discussion

The reactivities of **1**−**4** illustrate two novel processes in fundamental enediyne photochemistry. The first is the ability for copper coordination to promote photochemical Bergman cyclization while the uncomplexed ligand is unreactive under the same conditions. Coupled to this unusual result is the second intriguing aspect of the observed photo-Bergman reactivity, namely, the use of MLCT excitation as a conduit to cyclized product formation.

Photolysis of **1** with $\lambda \geq$ 395 nm in the presence of excess H-atom donor results in no reaction on either the NMR tube or preparative scales. Examination of the electronic absorption spectrum of **1** (Figure 1, Table 2) reveals that **1** has virtually no extinction at $\lambda >$ 300 nm, and thus would not be photoelectronically reactive at longer wavelengths. In contrast, both the Cu(I) and Cu(II) complexes, **2** and **3**, respectively, exhibit good yields of Bergman-cyclized product (**5**, **6**) upon photolysis with $\lambda \geq$ 395 nm. In either case, both bound enediyne ligands are determined to have reacted (87% and 81% yields from **2** and **3**, respectively, on the basis of stoichiometric analysis of the demetalated organic products extracted following photolyses, as well as the characterization of the inorganic photoproduct **5**.

The determination that both enediyne ligands bound to copper are Bergman-cyclized following photolysis leads to intriguing questions about potential photochemical mechanisms by which these photoreactions occur. Excitation of both **2** and **3** with $\lambda \geq$ 395 nm accesses MLCT absorption bands (MLCT for **2**, LMCT for **3**) of π-character. Using Table 2, and the ΔE(redox) approximation to estimate the charge-separated state energies upon electron transfer between the metal−ligand HOMO and LUMO,[112] the Cu(I)−L$^{\bullet+}$ (1.77 eV) and Cu(II)−L$^{\bullet-}$ (1.95 eV) species are thermodynamically accessible via the $\leq$3.14 eV excitation energy. However, preparative-scale photoreactions of

(110) Breiner, K. M.; Daugherty, M. A.; Oas, T. G.; Thorp, H. H. *J. Am. Chem. Soc.* **1995**, *117*, 11673−11679.
(111) Pogozelski, W. K.; Tullius, T. D. *Chem. Rev.* **1998**, *98*, 1089−1108.
(112) Vlcek, A. A. *Electrochim. Acta* **1968**, *13*, 1063−1078.

Scheme 5. Triplet-Sensitized Photolysis of Zn(bpod)$_2$(CH$_3$COO)$_2$ (**4**)
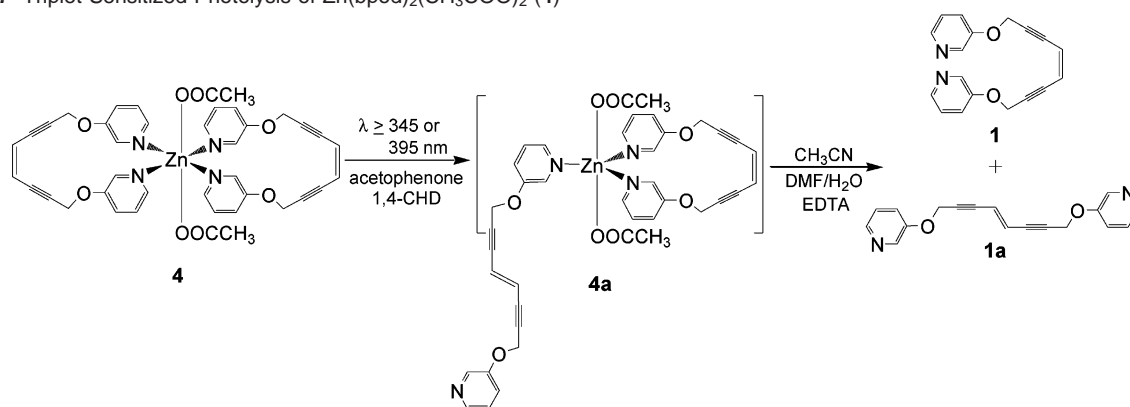
2 and **3**, as well as NMR-scale photolyses of **2**, reveal no detectable formation of redox-derived Cu(II) (from **2**) or Cu(I) (from **3**) photoproducts. In addition, cyclization of both enediyne ligands bound to the same copper center rules out an irreversible, intramolecular redox reaction. Photolysis of the Zn(II) complex **4** in the presence of excess Cu(NO$_3$)$_2$ or Cu(CH$_3$CN)$_4$PF$_6$ also does not lead to the generation of Bergman-cyclized photoproducts, indicating that cyclization is not derived from either free copper or a trace-metal-induced redox reaction. Finally, bulk electrolysis of **3** at 2.20 V failed to give clean conversion to a single species and, by NMR analysis, yielded a complex mixture devoid of the characteristic resonances of the Bergman-cyclized product. Although our findings are consistent with the redox lability of the enediyne moiety, taken together, these results suggest that photo-Bergman cyclization of **2** and **3** does not result from irreversible, metal-enediyne-localized photoredox chemistry. Our observations are consistent with redox lability of alkyne[87] or enediyne compounds,[43] but the inability of the latter to generate Bergman-cyclized product upon electrochemical oxidation.[43]

Insight into the photoreactivities of **2** and **3** can be gained from the photochemistry of the Zn(II) analogue **4**. Figure 1 (Table 2) reveals that **4** has almost the identical electronic spectrum as **1** (i.e., no CT transitions) and, thus, the same inertness to direct electronic excitation at $\lambda \geq 320$, 345, or 395 nm. However, these results do not preclude photoreactivity of **4** (or **1**). Many simple enediynes are known to be photochemically reactive either by direct photolysis with $\lambda < 320$ nm,[21,22,33,113] or by an energy-transfer mechanism.[22] Under these conditions, three types of photoreaction pathways predominate, namely (i) the formation of Bergman-cyclized product via $^1\pi-\pi^*$ excitation, (ii) reduction of an alkyne unit to yield dien-yne species upon $^3\pi-\pi^*$ population,[22] or (iii) cis−trans isomerization of the ethylene unit in the absence of an annulated skeleton.[114]

The photochemical inertness of **4** to direct excitation for $\lambda \geq 320$ nm provides an opportunity to use photoinduced triplet energy transfer to activate the enediyne moiety, and to investigate the product obtained via ligand-centered triplet population. Excitation of a triplet sensitizer (acetophenone; $E_T = 3.21$ eV)[115]

in the presence of **4** leads to formation of the *trans*-bpod enediyne species (*t*-bpod, **1a**) that is bound to Zn(II) (**4a**, Scheme 5) via bimolecular triplet−triplet energy transfer. Identification of the product is confirmed by demetalation with EDTA and spectroscopic comparison to authentic **1a** (Scheme 1). Although not isolated and characterized as a Zn(II) complex, coordination of the product to the metal is determined by thin-layer chromotography and NMR shifts relative to authentic, unbound **1a**. These results show that ligand-localized $^3\pi-\pi^*$ excitation ($E_T \approx 3.12$ eV)[27] of a closed-shell enediyne leads to cis−trans isomerization about the ethylene unit, which has been described both theoretically[27] and experimentally.[114]

Because neither redox-initiated Bergman cyclization nor $^3\pi-\pi^*$-derived products are detected upon the photolysis of **2** or **3**, and because both photoreactions generate comparable yields of cyclized product whereas the free ligand **1** is inert under the same conditions, the photochemical pathways by which these copper metalloenediynes perform Bergman cyclization can only be considered to be atypical. This is especially apparent in light of the photosensitized photolysis of d^{10}, diamagnetic **4**, which yields traditional $^3\pi-\pi^*$ product as observed for simple organic enediynes.[114] In this sense, the Zn(II) center in **4** serves a structural role in drawing the alkyne termini into closer proximity for cyclization, as evidenced by the moderate DSC temperature for the complex (163 °C), relative to other metalloenediynes.[34,35,39,116] Energetically, this lowers the barrier to enediyne cyclization but, from an electronic excited-state perspective, the diamagnetic d^{10} metal center is essentially an innocent spectator and, thus, does not influence the character of the excited electronic manifold.

In contrast, the role of the copper centers in the Bergman cyclization of **2** and **3** is markedly different. Although difficult to verify experimentally, plausible mechanistic avenues can be proposed by considering established photochemical properties of Cu(I) and Cu(II) bis- or dipyridyl complexes.[95−102] For the Cu(I) complex **2**, the d^{10} electronic configuration and redox activity of the metal center leads to partial one-electron, MLCT promotions from the metal dπ orbitals to the empty π^* orbitals of the pyridine ring,[101,102] which generates the ^{3}MLCT state[102] rapidly via spin−orbit coupling. Free rotation of the pyridine rings relative to the enediyne unit, combined with the lower-lying π orbitals of enediyne motif (Table 1), permit delocalization of the excited state onto the enediyne fragment through

(113) Choy, N.; Blanco, B.; Wen, J.; Krishan, A.; Russell, K. C. *Org. Lett.* **2000**, *2*, 3761−3764.
(114) Kagan, J.; Wang, X.; Chen, X.; Lau, K. Y.; Batac, I. V.; Tuveson, R. W.; Hudson, J. B. *J. Photochem. Photobiol., B* **1993**, *21*, 135−142.
(115) Turro, N. J. *Modern Molecular Photochemistry*; The Benjamin/Cummings Publishing Company, Inc.: Menlo Park, CA, 1978.

(116) Rawat, D. S.; Zaleski, J. M. *Chem. Commun.* **2000**, 2493−2494.
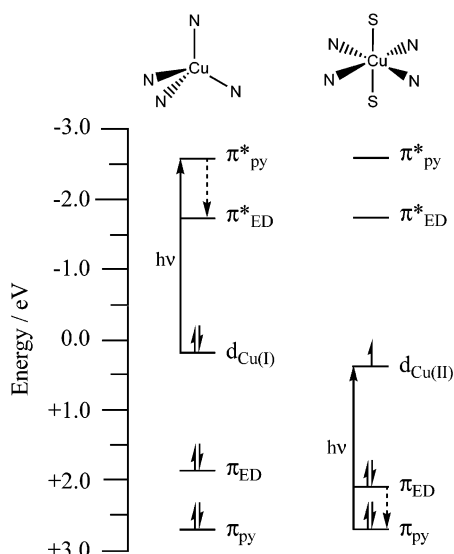
Figure 4. Relative energies of copper and ligand frontier orbitals and their involvement in the photoelectronic Bergman cyclization reactions of **2** and **3**.

the π-system (Figure 4). Although not equivalent to activating the enediyne unit for reactivity via an electrochemical redox reaction,[43] this Dexter-type (exchange)[117] energy-transfer mechanism,[44,118,119] which is analogous to ligand-field[118] or charge-transfer-to-intraligand[45,120,121] excited-state quenching, could induce small but sufficient geometric perturbation to permit Bergman cyclization. Thus, the photoreaction could be viewed as occurring through an enediyne-centered state, despite initial population of the formal Cu-pyridine CT manifold.[122] Charge-transfer-to-intraligand photochemical dynamics of this type are uncommon but not unprecedented.[120,121,123,124] On the basis of the lack of a strongly radiative chromophore, and the absence of prominent dipole-allowed absorption bands for **1** at $\lambda > 300$ nm, a unimolecular exchange energy-transfer mechanism is very plausible.[44,118,119] However, because of the mixed-spin character of the CT excited states, and their ability to interact with ligand-centered singlet/triplet states, a Förster singlet energy-transfer scheme cannot be completely ruled out.[123]

Photolysis of the d[9] Cu(II) complex **3** with $\lambda \geq 395$ nm leads to charge transfer from the pyridine π-orbitals to the empty hole in the $d_{x^2-y^2}$ orbital ([2]LMCT), creating a partial π-hole on the bound pyridine moiety. The modest enediyne oxidation potential is reflective of high-energy π-orbitals containing considerable enediyne character that could serve as a thermodynamically accessible site for excited-state–partial-hole transfer onto the enediyne unit (Figure 4). Such electronic modulation could generate sufficient geometric distortion to promote Bergman cyclization. The details of these distortions, as well as the potential influence of ^{2}CT vs $^{1,3}\pi-\pi*$ excited states, are currently under investigation.

The triplet energy-transfer-derived isomerization of the bpod ligand bound to Zn(II) in **4** is consistent with previous energy-transfer studies of enediynes,[22,114] and density functional theory (DFT) calculations for nonbenzannulated structures.[27] Excited states derived from a molecular-orbital approach using ethylene and acetylene fragments are thermodynamically ordered such that the lowest-energy triplet state is localized on the double bond and is of $\pi-\pi*$ parentage.[27] Population of this state by bimolecular Dexter energy transfer would be expected to lead to the isomerized *trans*-enediyne product, as observed for **4**.

In addition to the fundamentally intriguing photochemistry of these metalloenediynes, the abilities of **2** and **3** to effect DNA degradation by H-atom abstraction[65,110,125] rather than by the more-common base oxidation mechanism of inorganic agents are rare. At low concentrations of **2** and **3**, nicked DNA is prevalent, whereas at higher concentrations (>100 μM), an almost constant mixture of linear:nicked DNA exists that begins to approach 1:1. The low quantum yield for photoreactivity of **2** ($\phi_{366} = 4.2 (\pm 0.6) \times 10^{-5}$) suggests that the length of photolysis time is directly a result of the quantum efficiency and, as the moderate association constant of **3** ($K_m = 2.6 (\pm 0.2) \times 10^4$ M^{-1}) suggests, is not a result of poor binding to the DNA duplex.

The ^{32}P-labeled oligonucleotide results provide two important insights. First, the high-resolution gels confirm that the fundamental photochemical intermediate produced upon the photolyses of **2** and **3** reacts via H-atom abstraction and not base oxidation, which is consistent with the 1,4-phenyl diradical proposed in the formation of the Bergman-cyclized products. Moreover, introduction of free Cu^{2+} cations does not yield the cleavage pattern observed upon photoactivation of **3**, confirming that trace metals are not responsible for these results. Although no sequence specificity is observed for the photoreactivity of **3**, this is not surprising in the absence of any sequence-selective functionality. Second, the two-band pattern observed in Figure 3, as well as subsequent identification of the faster-migrating species as a 3′-phosphoglycolate, indicates that copper metalloenediyne **3** is indeed cleaving DNA by ribose degradation and not by base-centered, redox-induced strand scission. In the metalloenediyne field, photoelectronic H-atom abstraction reactivity has not been previously demonstrated. These results place **2** and **3** in a category with other H-atom-abstracting metal-based agents such as Fe^{2+}-bleomycin,[65] Rh-phi complexes,[66] and [Pt(pop)$_4$]$^{4-}$ (pop = P$_2$O$_4$H$_2^{2-}$),[110,125] of which there are a limited number of examples.

5. Conclusion

We have described the unique photoelectronic Bergman cyclization of metalloenediynes of Cu(I) and Cu(II) and shown that the intermediates perform double-stranded DNA cleavage. The photocyclization mechanism and consequential deoxyribose chemistry do not result from direct redox reactions with the metal centers, but rather are derived from the photoelectronic Bergman cyclization of the enediyne unit and subsequent C-4′ H-atom abstraction. The results show that metal–ligand charge-transfer transitions can serve as conduits for population of

(117) Dexter, D. L. *J. Chem. Phys.* **1953**, *21*, 836−850.
(118) Endicott, J. F. *Coord. Chem. Rev.* **1985**, *64*, 293−310.
(119) Ferraudi, G. F. *Elements of Inorganic Photochemistry*; John Wiley and Sons: New York, 1988.
(120) Yam, V. W.-W.; Lau, V. C.-Y.; Cheung, K.-K. *Chem. Commun.* **1995**, 259−261.
(121) Ford, P. C.; Wink, D.; Di Benedetto, J. *Prog. Inorg. Chem.* **1983**, *30*, 213−271.
(122) Time-dependent DFT calculations to evaluate the progression of the cyclization reaction along the excited-state reaction coordinate for **2** and **3** are ongoing and will be described in a future report.
(123) Boyde, S.; Strouse, G. F.; Jones, J. W. E.; Meyer, T. J. *J. Am. Chem. Soc.* **1989**, *111*, 7448−7454.
(124) Meyer, T. J. *Pure Appl. Chem.* **1990**, *62*, 1003−1009.

(125) Kalsbeck, W. A.; Gingell, D. M.; Malinsky, J. E.; Thorp, H. H. *Inorg. Chem.* **1994**, *33*, 3313−3316.

enediyne-localized excited states that lead to Bergman cyclization and, thus, diradicals capable of performing H-atom abstraction from the deoxyribose backbone of DNA. Overall, the study reveals a role that transition metals can play in influencing not only thermal metalloenediyne cyclization, but also in the photocyclization of metalloenediynes.